

For Assignment Help

Contact Us:

Email Us: essaycorp.aus@gmail.com

Whatsapp: <https://api.whatsapp.com/send?phone=12053509760>

Form: <https://form.jotform.com/223001844063444>

Website: <https://www.essaycorp.com/>

Study on mechanical response of loaded wing by using finite element computational modeling

Executive summary

The aim of the current work is to determine the deflections and stresses in a loaded Pilatus PC/9 wing using finite element computational modeling. The aircraft wing is modeled using 3D beam-shell representations and linear static analysis is performed with commercial finite element analysis package ABAQUS v6.14. Also, the surface-to-surface restraint being the main key for the simplification of computational model in the finite element analysis of complex structures such as the aircraft wing is described in details. Finally, finite element simulation results are compared with experimental results and some topics are discussed.

1. Introduction

Wing is the most important component of aircraft design because the wings are the main surfaces that support the aircraft by lifting in flight. Therefore, It has to be used the components that have high strength and stiffness at the wing structure of the airplane.

PC-9 is a single-engine, low-wing dual-seat turboprop training aircraft. Pilatus PC-9/A is two-seat turboprop aircraft as principal basic training aircraft of the Australian Defence Force. The PC-9 is best known to the public as the aircraft flown by the Air Force Roulettes in aerobatic displays at major events throughout Australia. Figure 1, Figure 2 and Figure 3 shows the global structure and section dimensions of the Pilatus PC-9 Aircraft wing, respectively.

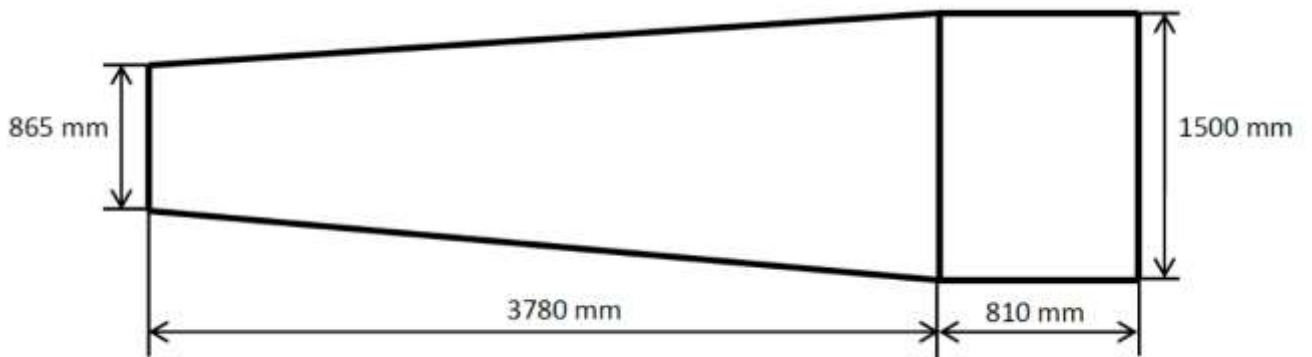
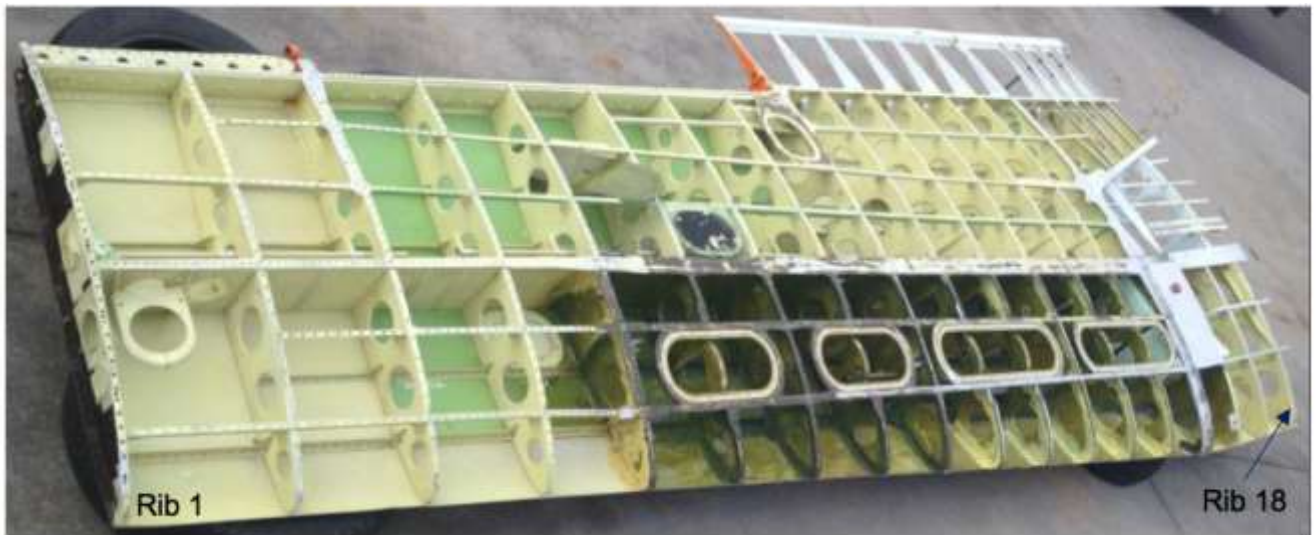


Fig1. PC-9 wing structure and global dimension

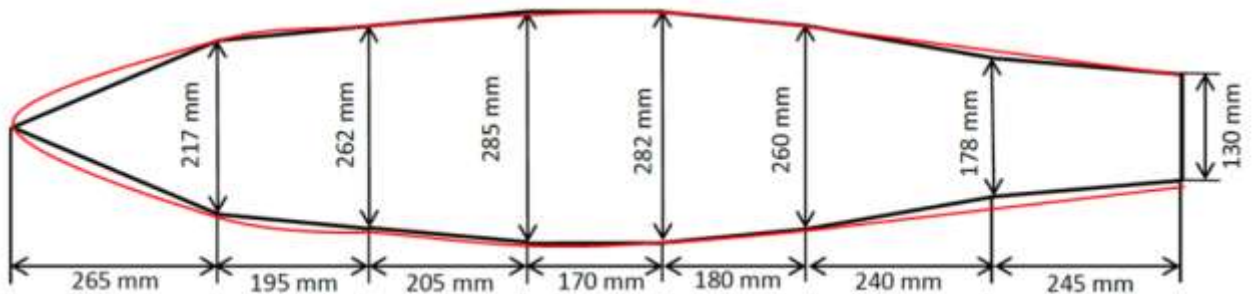


Fig2. Dimension of rib at PC-9 wing root

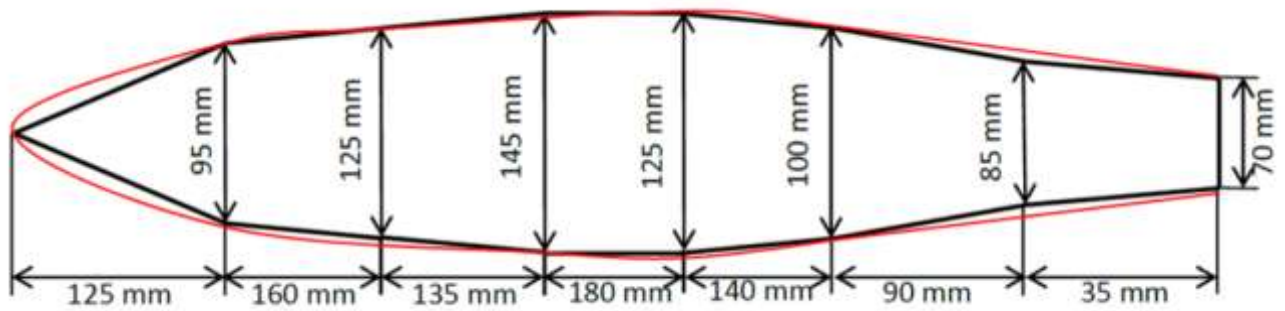


Fig3. Dimension of rib at PC-9 wing tip

In order to analyze the behavior of the wing, an experimental study was conducted. The experimental setup consists of a purpose built test rig for the Pilatus PC-9 wing, as illustrated in Figure 4. Two hydraulic actuators (equipped with a load cell), located at 2/3 span, was used to apply displacement while the wing root is clamped to the test bench, as shown in Figure 4. Strain gauges were used to record the applied strain at the root of the wing. But manufacturing the product for experiment costs great times, cares and materials.



Hydraulic Actuators at 2/3 Span



Clamped Wing Root

Fig4. Experiment setup

In order to reduce such cost, numerical simulation methods have appeared. Among them, the most representative method is FEM. Finite element method (FEM) is very powerful numerical calculation method for design and numerical analysis of engineering structures as well as simulation of natural phenomena. It was developed many commercial software packages based on finite element method such as ABAQUS, ANSYS and ADINA etc before a few decade and at recent years, they are being used successfully at design and strength estimation of very complex structures such as aircraft wing at

aerospace industries. Computer aided engineering analysis based on the finite element scheme is recognized to be a great effective numerical simulation and optimization technique in the field of aircraft design. It has important guiding significance and engineering value that can advance product qualities and performance, decrease production costs; shorten design cycle, and so on. FE modeling is data pre-processing for FE analysis. The calculation correctness of the FE method depends on the level of approximation of physical characteristics of the model and its real structure. Therefore, establishing a correct and suitable FE model is the most important issue to perform finite element numerical simulation and optimization.

In three-dimensional finite element analysis of the structures such as the aircraft wing, the main key for the simplification of computational model is to apply the surface-to-surface restraint suitable for the contact pairs of three-dimensional shell element. ABAQUS provides some methods in order to restraint three-dimensional shell-to-shell and shell-to-beam elements [19].

- **Tie restraint formulation based on surface**

Abaqus uses the below criteria to determine which slave nodes will be tied to the master surface.

Abaqus then forms restraints between these slave nodes and the nodes on the master surface.

Abaqus use surface-to-surface method and node-to-surface method to generate the coefficients.

When analysis process performed using Abaqus/Standard product is imported into Abaqus/Explicit product, the tie restraints are not imported and need to be redefined. If the imported analysis is a continuation of the initial analysis significantly, it is an important problem that tie restraints has to be as similar as possible.

Then, it needs to be used the similar restraint type necessarily. If in the original Abaqus/Standard analysis, the initial method was used, the surface-to-surface method should be specified in the Abaqus/Explicit analysis. Similarly to above, if in the original Abaqus/Explicit analysis the initial method was used, node-to-surface method should be specified in Abaqus/Standard analysis.

The numerical noise for tied interfaces involving mismatched meshes are minimized the surface-to-surface method. The surface-to-surface method enforces restraints in an average sense over a certain region unlike in the original node-to-surface method, other while it enforces restraints at discrete points.

In Abaqus/Standard, the surface-to-surface method is used by origin with exceptions noted below, and it is optional in Abaqus/Explicit. The cost of the surface-to-surface method can be quite important for the case of infinite acoustic elements tied to shell elements in Abaqus/Standard and therefore, in this case the node-to-surface method is used by original.

The surface-to-surface method ordinarily includes more master nodes rather than the node-to-surface method per restraint. It tends to increase the solver bandwidth in Abaqus/Standard and, therefore, can increase response cost. The extra cost is fairly small in most applications but can become important in some cases. In the following parameters, it really can lead to the surface-to-surface method:

- A great fraction of tied nodes (DOF) in the model
- The master surface being more refined than slave surface
- Multiple layers of tied shells, such that the master surface of one tie restraint acts as the slave surface of other tie restraint.

surface of other tie restraint.

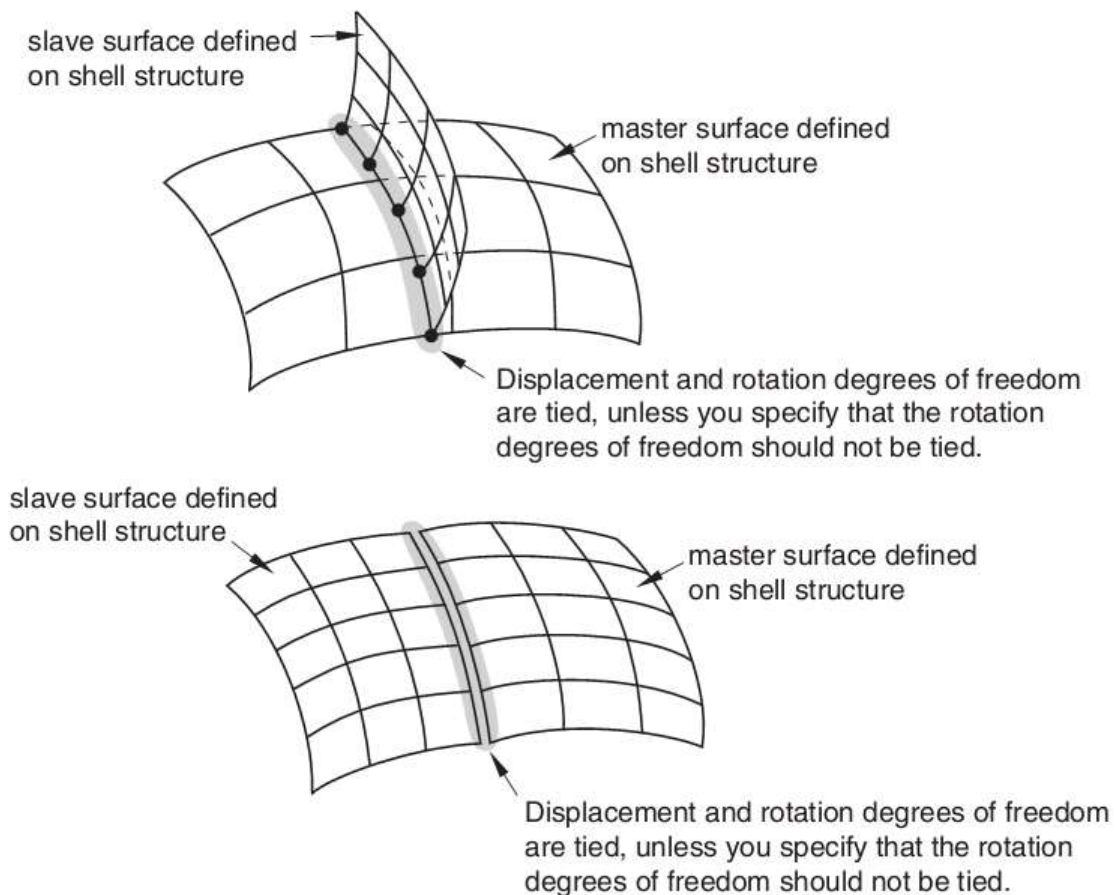


Fig5. Surface-based tie algorithm

It is sited the coefficient equal to interpolation functions at that point where the slave node projects onto that master surface in the original node-to-surface method, which is used by original in Abaqus/Explicit and optional in Abaqus/Standard. This method is more effective anywhere for complex surfaces.

- **Choosing the master/slave surfaces at a surface based tie restraint**

The choice of master/ slave surfaces can be affected importantly on the accuracy of the response, especially in the case if the node-to-surface method is used. But in the case of the surface-to-surface method the effect is great less and the accuracy ordinary. In each of two cases, if two surfaces in a contact pair are deformable surfaces, in order to achieve the best accuracy the master surface should be chosen as the surface with coarser meshing.

In Abaqus/Standard a rigid plane cannot to be used as a slave surface in tie restraint. Following with this criterion, the capability to resolve over restraints in Abaqus/Standard will change tie restraint definitions in the below cases:

- Tie restraints between two surfaces of the similar rigid body are killed.
- Tie restraints between two surfaces of two rigid bodies are replaced by a BEAM-type connector between the respective rigid body refer nodes.
- Tie restraints specified with a purely rigid slave surface and a purely deformable master surface are modified to reverse the master and slave assignments unless this is not possible due to other modeling restrictions (in which case an error message is issued).

If the slave surface that you specified is partially rigid and partially deformable, these methods are not applied and therefore, Abaqus/Standard issues an error message in such cases. If two media have different wave speeds, the optimal meshes for each of the media will have different characteristic element lengths. In other words, the faster medium will have larger elements. If surfaces of these meshes are used in a tie restraint, the surface of the finer mesh of the slower medium should be designated as the slave. Nevertheless, in the region near the tied surfaces, the physical wave phenomena in both fast and slow media will typically have length scales characteristic of the slower medium; that is, of the shortest length scale in the physical problem. Therefore, if these phenomena are important, the mesh of the faster medium should be refined to the scale of the slower medium in the

vicinity of the contact region.

- **Defining the surfaces and a tie restraint for a pair of surfaces**

By original, nodes are tied only where the surfaces are close to one another. One surface in the restraint is designated to be the slave surface, while the other surface is the master surface. A name must be assigned to this restraint and may be used in post-processing with Abaqus/CAE. A surface-based tie restraint can be used to make the translational and rotational motion as well as all other active DOF equal for a pair of surfaces.

As the slave surface, it also can be used either element-based or node-based surfaces. Any surface type (element-based, node-based, or analytical) can be used as the master surface. It may need to take some surface restrictions into consideration depending on which tie formulation is used and whether the analysis is conducted in Abaqus. Two tie formulations are available: the surface-to-surface formulation, which is used by original in Abaqus/Standard, and the more original node-to-surface formulation.

The surface-to-surface formulation ordinarily avoids stress noise at tied interfaces. The surface-to-surface formulation does not allow for a mixture of rigid and deformable portions of a surface, and the master surface must not contain T-intersections. Any nodes shared between the slave/master surfaces will not be tied with the surface-to-surface formulation.

- **Specifying the subset of slave nodes to be constrained**

Abaqus is using a position tolerance criterion to determine the constrained nodes based on the distance between the master nodes and the slave surface. Alternatively, regardless of their distance to the master surface it can be specified a node set containing the slave nodes to be constrained. The original position tolerance criterion ensures that nodes are tied only where the slave/master surfaces are close to one another in the initial configuration.

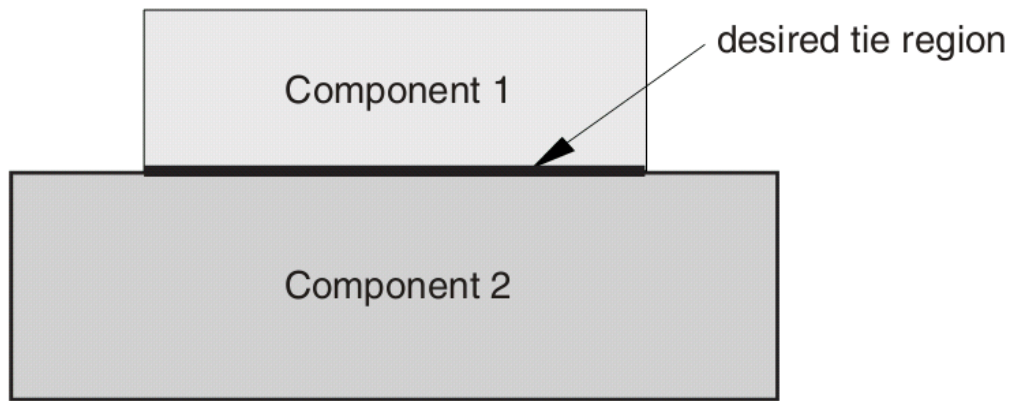


Fig6. Two components to be tied together

As seen from the Figure 6, these two surfaces in a tie restraint can be used as the slave/master surfaces to tie the two components in the desired region because it is tied only the nodes at the initial interface between the two surfaces. The original value of the position tolerance, d_{tol} , typically results in desired tie restraints with little effort. At below, it is provided details regarding the calculation of distances between surfaces and original values of the position tolerances. If desired, the position tolerance can be modified.

The factors such as shell thickness, surface-to-surface or node-to-surface restraint formulation, types of surfaces involved (element-based, node-based, or analytical) influence the calculation of the distance between surfaces for a particular slave node.

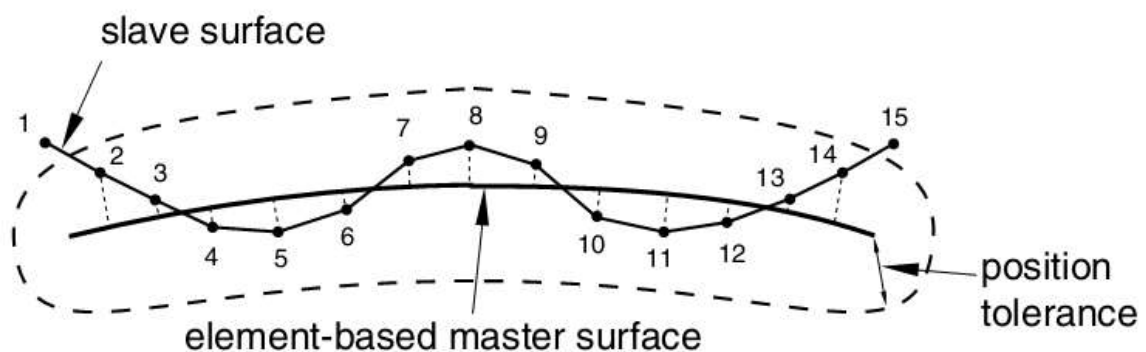


Fig7. Tolerance region around an element-based master surface with no thickness

Figure 7 shows the example of tolerance region around an element based master surface with no thickness. In Figure, nodes 2~14 satisfy the position tolerance rule for the node-to-surface and surface-to-surface restraint formulations. Line connecting nodes 1 and 2 and the line connecting nodes 14, 15 that is essential parts of the end slave segments are within the position tolerance shown, so 1

and 15 would also satisfy the position tolerance rule for the surface-to-surface restraint formulation except for the fact that the angle between the slave/master surfaces is greater than 31° at these locations.

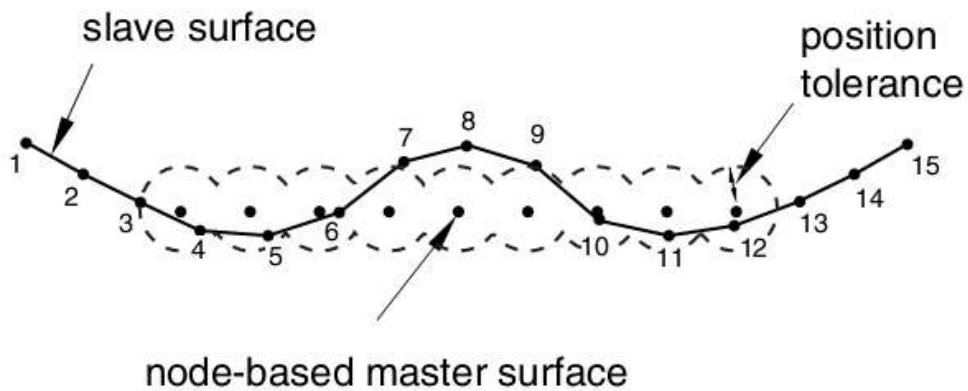


Fig8. Tolerance region around a node-based master surface with no thickness

Figure 8 shows the example of tolerance region around an node based master surface with no thickness. In other words, it shows how the tolerance zone is defined around a node-based master face. The surface-to-surface restraint formulation reverts to the node-to-surface restraint formula for a node-based master surface. The distance between the surfaces for a respective slave node is based on closest master node and the original position tolerance for a node-based master surface is based on the mean distance between nodes in master surface. If the distance is less than the position tolerance, Abaqus will create a tie restraint between the slave node, the closest master node, and then, other master nodes in like proximity to the slave node. The distance between slave/master nodes can be much larger than the “normal” distance between the interfaces for mismatched meshes across tied surfaces, which can lead to confusion when using a position tolerance rule with a node-based master surface.

5% or 10% of the typical slave facet diagonal length for the surface-to-surface and node-to-surface tied formulas can be used to the original position tolerance for tie restraints between an element-based slave surface and an analytical rigid master surface is. The original position tolerance for tie restraints between a node-based slave surface and a master surface being analytical rigid is 6% of the typical distance between slave nodes. If it is used an analytical rigid master surface, the distance between interfaces for a particular position on the slave surface is based on the closest point on the master surface.

- **Overview of unrestrained nodes in tie restraint pairs**

Unless slave nodes are included in the tied node set or within the tolerance distance from the master surfaces at the early stage of the simulation, as discussed prior, Abaqus does not restrain them to the master surfaces. Any slave nodes not satisfying these criteria will remain unrestrained for the duration of the analysis and they will not interact with the master surface as part of the tie restraint. In mechanical analysis, unless contact is defined between the slave/master surfaces, an unrestrained slave node can penetrate the master surface freely.

For each tie restraint pair, Abaqus creates a node set contain slave nodes that will be remain unrestrained and a node set comprising slave nodes that will be tied. Those node sets are available for post-process in Abaqus/CAE and they are listed as internal node sets. In the case of creating the model with surface-based tie restraints, it is very essential to use the information provided by Abaqus to identify any unrestrained nodes and to make any necessary changes at modeling to restrain them.

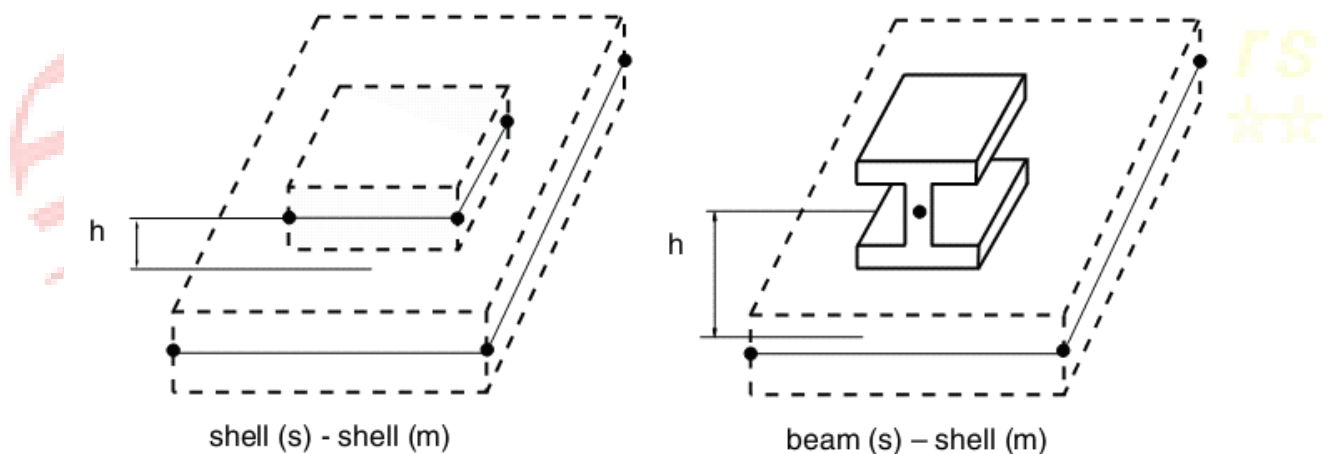


Fig9. Tie restraints to be applied between surfaces based on element types

Figure 9 shows some cases where an offset between the ref surfaces may be desirable for tied surface pairs to consider the shell or beam thickness. Abaqus allows a gap to exist between tied surfaces and these gaps may exist if it prevent nodal controls for tied surfaces. A gap between the ref surfaces may remain due to the presence of shell thick even if nodal controls are performed.

- **Constraining a surface of a 3D beam**

The surface based on 3D beam elements can be defined as the master surface for a tie restraint. In the case, each slave node is projected onto line formed with the nodes of the beam elements in the original configuration to show the projection position. During the next simulation, each slave node and

its projection point are connected by a rigid beam and the motion of each slave node is rigidly restrained to ones (translation and rotation) of its projection position. Modeling of interactions between the surface of a (complex) beam section and its surroundings can be done by allowing constraining other elements to a beam element-based master surface, without having to model the beam with continuum and/or shell elements. It is noted that Abaqus currently does not advice master surfaces based on any beam elements.

- **Adjusting the surfaces and considering offsets**

In Abaqus, the slave nodes to be tied in the original configuration without causing strain to resolve gaps such that the surfaces are just touching, accounting for any shell thickness (unless it have specified that thick should not be considered, as discussion prior in the context of the position tolerance rule) but not considering for beam or membrane thickness are automatically repositioned. The cases that no adjust are made where tied faces are closer with than the composed half-shell thickness, are except. All processes are controlled such that the slave/master surfaces are never pushed apart. For example, the original surfaces will only become closer as result of the controls. The recommend is that it allows automatic controls to occur, specially if other surface has rotations. In that case a consistent offset vector is used and so in correct behavior of the restraint under rigid body rotation can occur when slave nodes are not lying exactly on the master surface. If the slave surface belongs to a substructure or when either the slave or master surface is a beam element-based surface, controls are not made. In the latter cases it should be located the beam element nodes with the desired offset from the other surface.

If both of the following conditions are met, a slave node is countered for control:

- Whatever rule is in affect for generating a restraint (either because it satisfies the position tolerance rule or belongs to the specified node set of restrained slave nodes, as prior discussion), the slave node satisfies.
- Accounting for any offset o f the element reference surfaces from the respective element mid surfaces, the slave node is more than the composed thickness of the slave/master surfaces away from its projection point on that master reference surface.

Nodal controls for tie restraints are processed sequentially in the order of the restraint definitions

at the start of an analysis. If different restraint or contact definitions involve the same nodes, some controls may cause lack of compliance for contact or restraint definitions that were previously processed.

Using a surface-based tie restraint in Abaqus alternate defining tied contact has next advantages:

- DOF of the slave surface nodes will be eliminated.
- Rotational DOF as well as directional DOF can be tied.
- Because master surface nodes are associated with respective slave node, the tie restraint is more effective in terms of amount of the fronts of the operator matrix.

• Because they allow the use of ordinary surfaces, tie restraints are great more general.

• It also considers surface offsets and shell thickness.

Other while, for the tie restraints, the below limitations exist:

• It cannot be used surface-based tie restraints to connect gasket elements that model thick direction behavior only.

• A rigid surface cannot use as a slave surface in a restraint pair in Abaqus.

• In Abaqus a slave node of a tie restraint cannot to be used as a slave node of another restraint.

• Tie restraints cannot be used to tie infinite elements to finite elements in Abaqus. To couple in finite and finite elements in Abaqus, elements must share the nodes.

• The axisymmetric solid Fourier elements with nonlinear, asymmetric deformation cannot form element-based surfaces; therefore, such surfaces cannot be used in tie restraints.

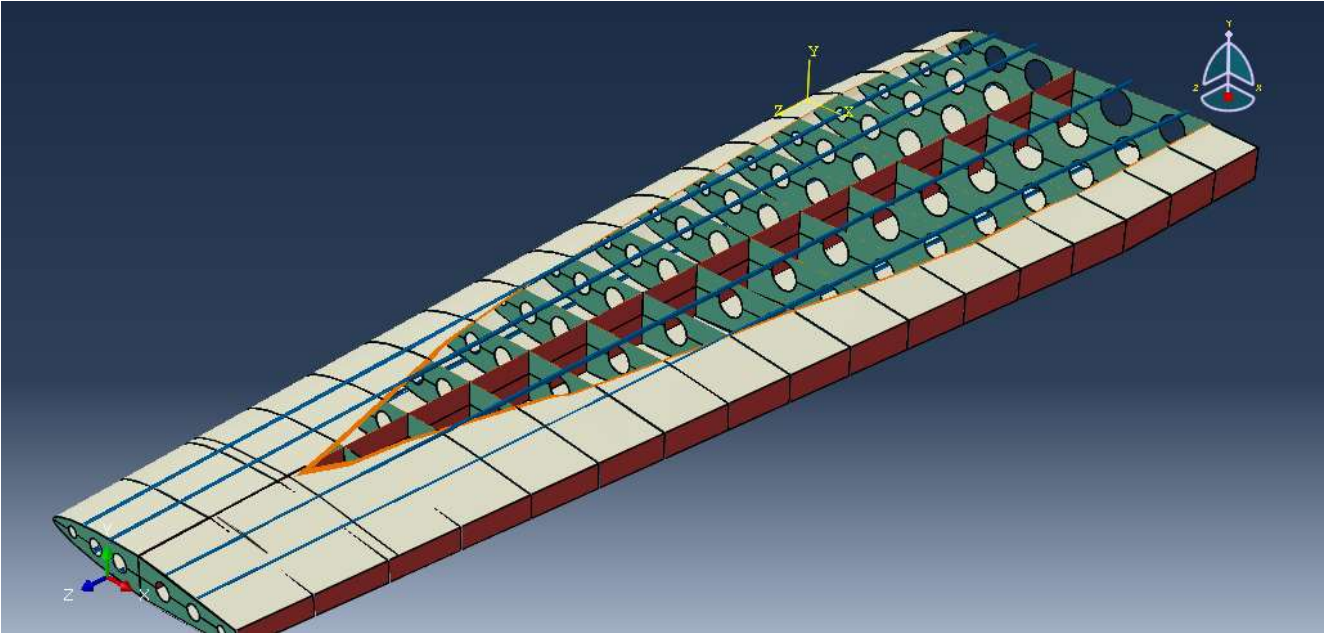
Here, complex structural components of wing structure are modeled by individual three-dimensional shell parts by using the surface-to-surface restraint function for the contact pairs of ABAQUS as discussed above and then they are cooperated into the whole structural analysis. Moreover, based on the modeling capacity of ABAQUS/CAE, more effective method combined with Solidworks is chosen, leading to the improvement of computational effect by applying the element size and element shape suitable for the linear elastic analysis [20].

The finite element simulation results is compared with the supported experimental data and some factors that influences on the deflection of wing as well as the numerical error are evaluated.

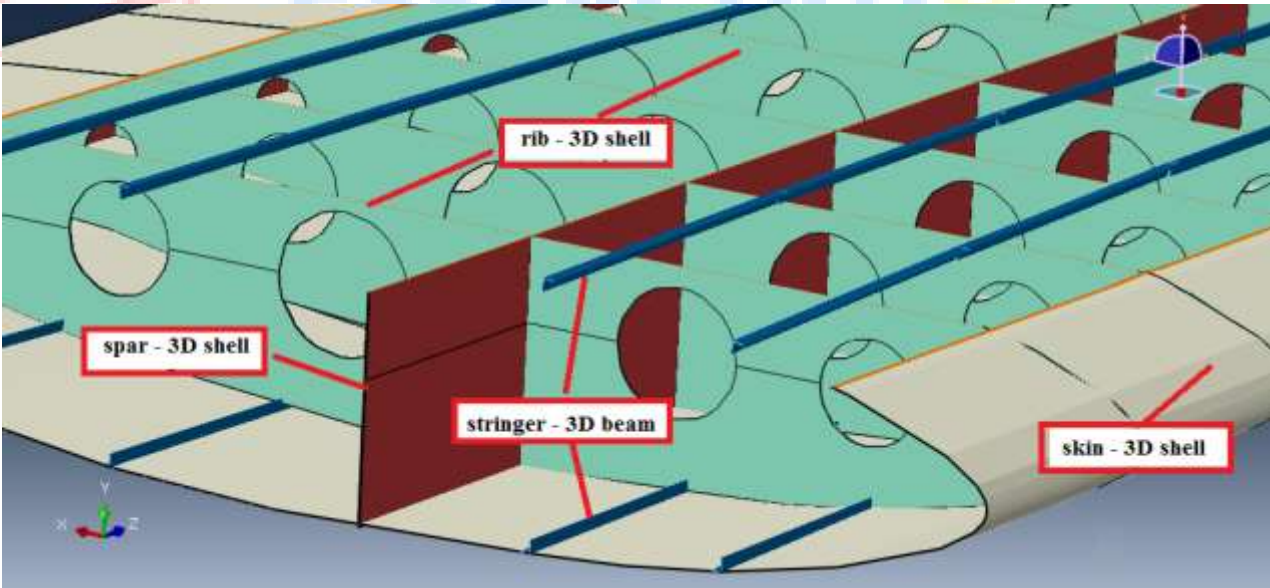
2. Engineering analysis

2.1. The review of PC-9 wing finite element modeling.

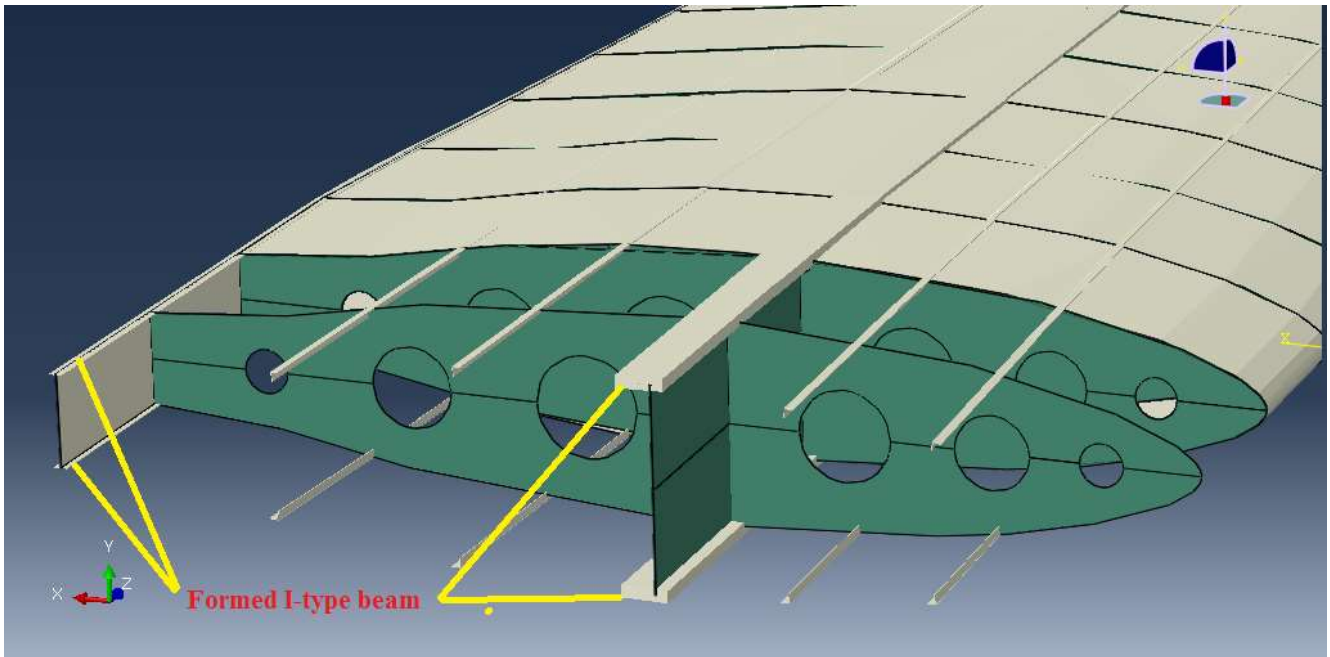
Figure 10 shows the FE model for PC-9 wing structure made by using commercial Finite element software ABAQUS 6.14.



a)



b)



c)

Fig10. FE model of PC-9 wing structure a) Appearance of PC-9 wing FE model, b) Inner structure of the wing, c) Formed beam for I-type spar

Wing consists of skin, rib, spar (front and rear) and stringer as shown from the figure 9. The skin makes the appearance of the wing and is connected to stringer. It transfers aerodynamic distributed load to stringers. The rib puts into the direction of air flow and sustains stringers and skin so that maintains the type of section. The spar is main member of wide direction at the wing framework and carries out shearing force and bending moment. These members carry out shearing force and bending moment and are modeled as 3D shell. The stringer puts into length direction of wing and is modeled as 3D beam. Figure 10 shows the inner structure of wing with all components.

2.2. Modeling process

Firstly, geometric models of rib and skin are generated by Solidworks (or other CAD package) manually, and then imported in ABAQUS/CAE.

Note: It can make the FE model of the wing structures directly by using only ABAQUS/CAE, but there are some problems, namely it can induce the bad finite element mesh. Figure 11 shows the FE model only by using ABAQUS/CAE and Figure 12 shows the bad finite element mesh state. Thus, it is used FE modeling by using ABAQUS/CAE with Solidworks in this work.

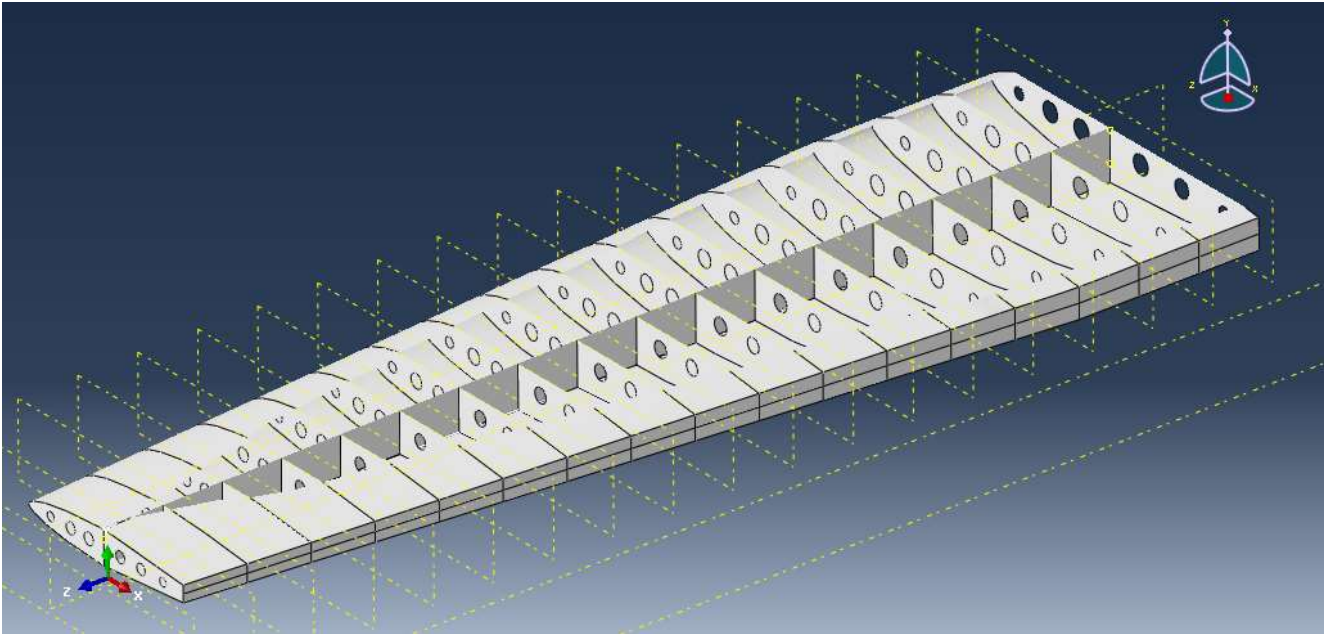


Fig11. FE model only by using ABAQUS/CAE

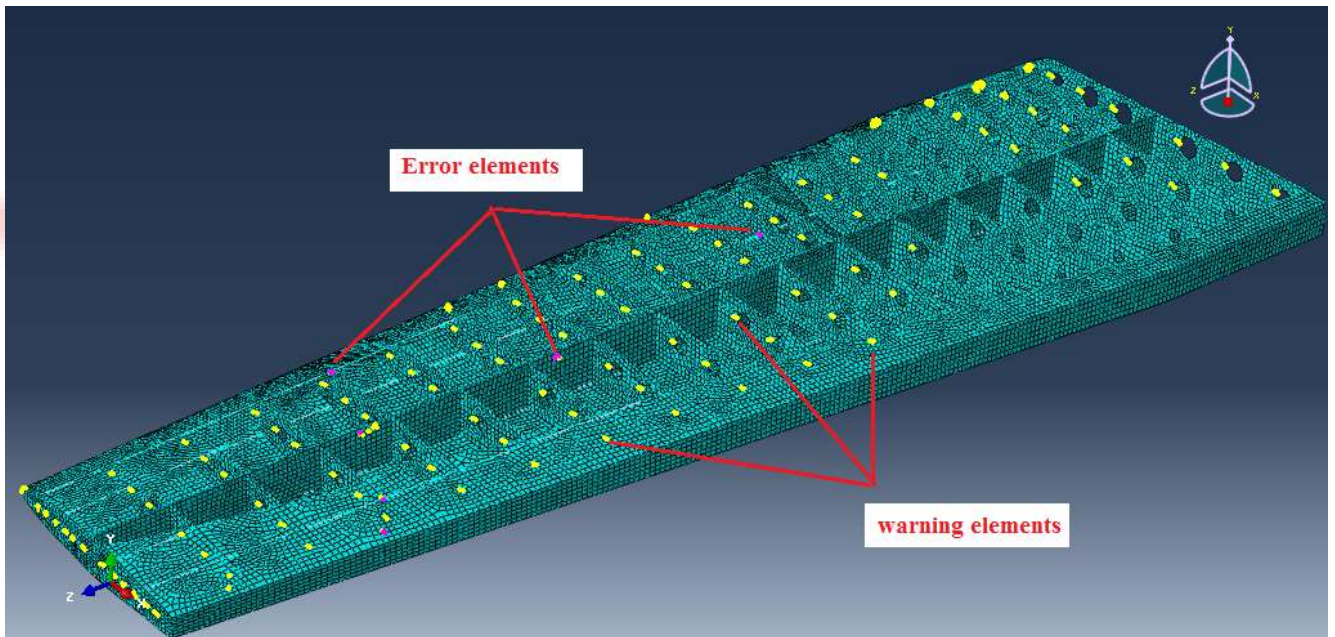


Fig12. Bad meshing on FE model only by using ABAQUS/CAE

Secondly, in **Part** module, make the geometry model of the stringers using 3D wire and datum plane (and points) on wing skin.

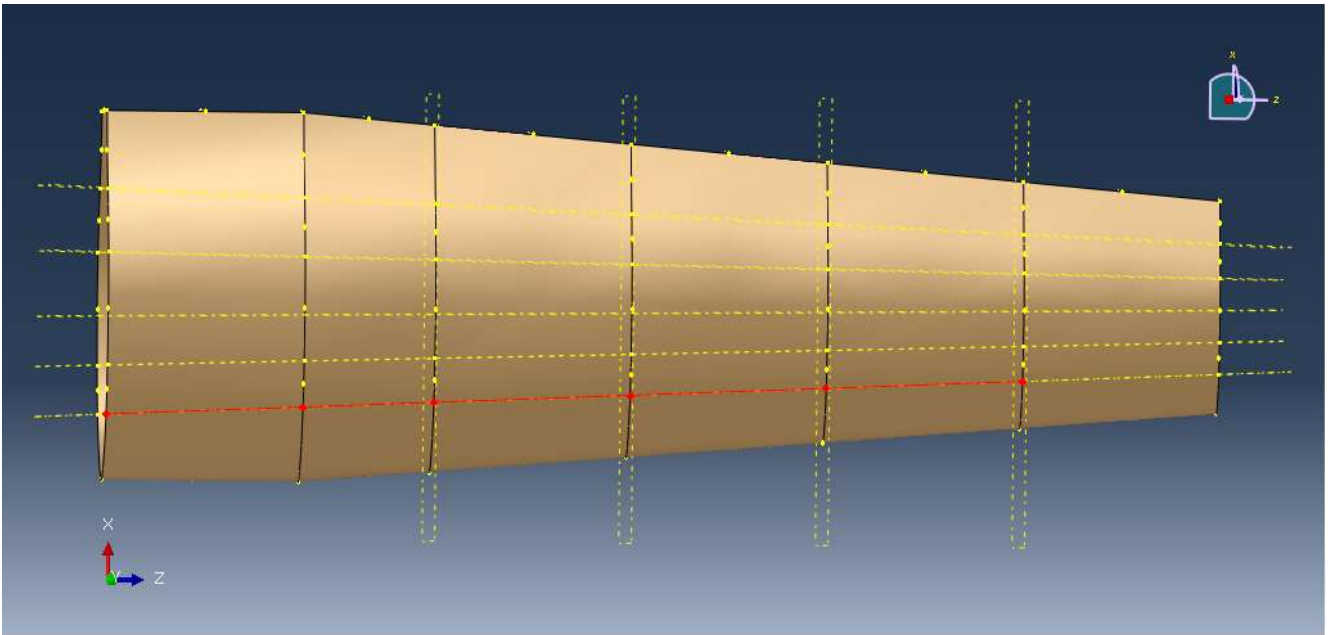


Fig13. Making the stringers on wing skin

Thirdly, in **Assembly** module, merge the 18 ribs and front spar (to easy the meshing and restraint of whole structure).

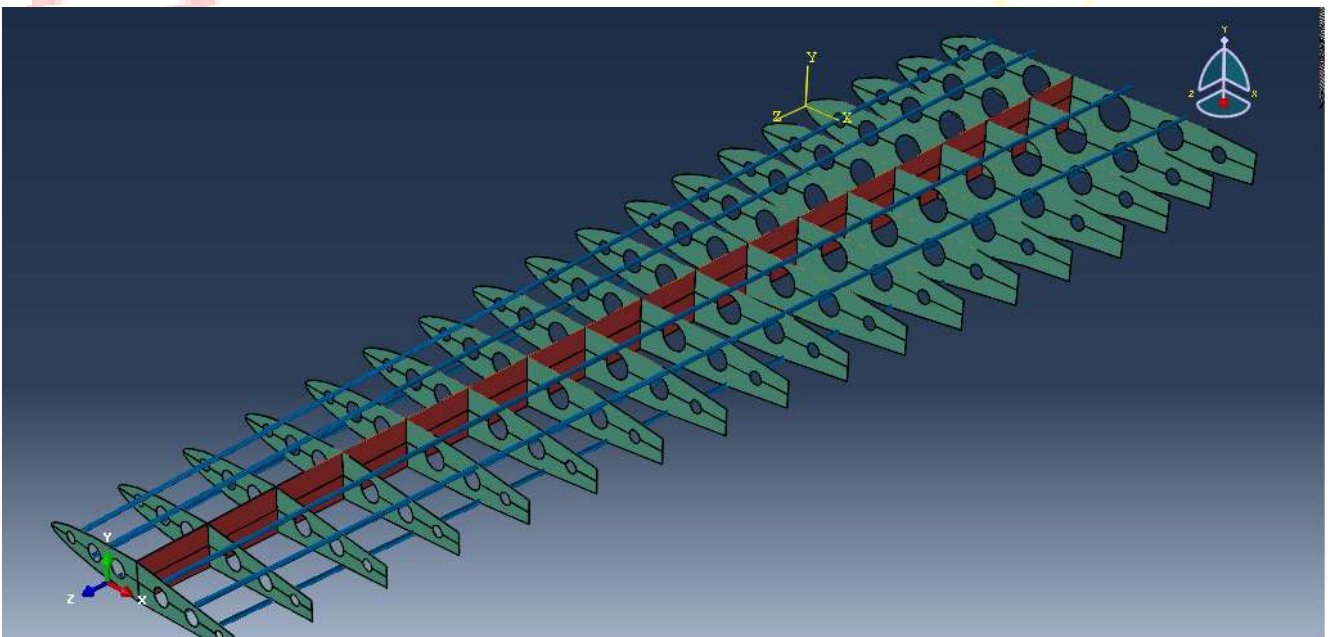


Fig14. Part merged from the 18 ribs and front spar

Fourthly, in **Property** module, create the material properties and sections; assign the sections on the structure components. The material used here is the aluminium 2024. Its Young's modulus and Poisson's ratio is 9.6×10^6 MPa and 0.36, respectively.

Fifthly, in **Assembly** module, assembly whole parts of rib, skin, and stringers as can see from

Figure 15.

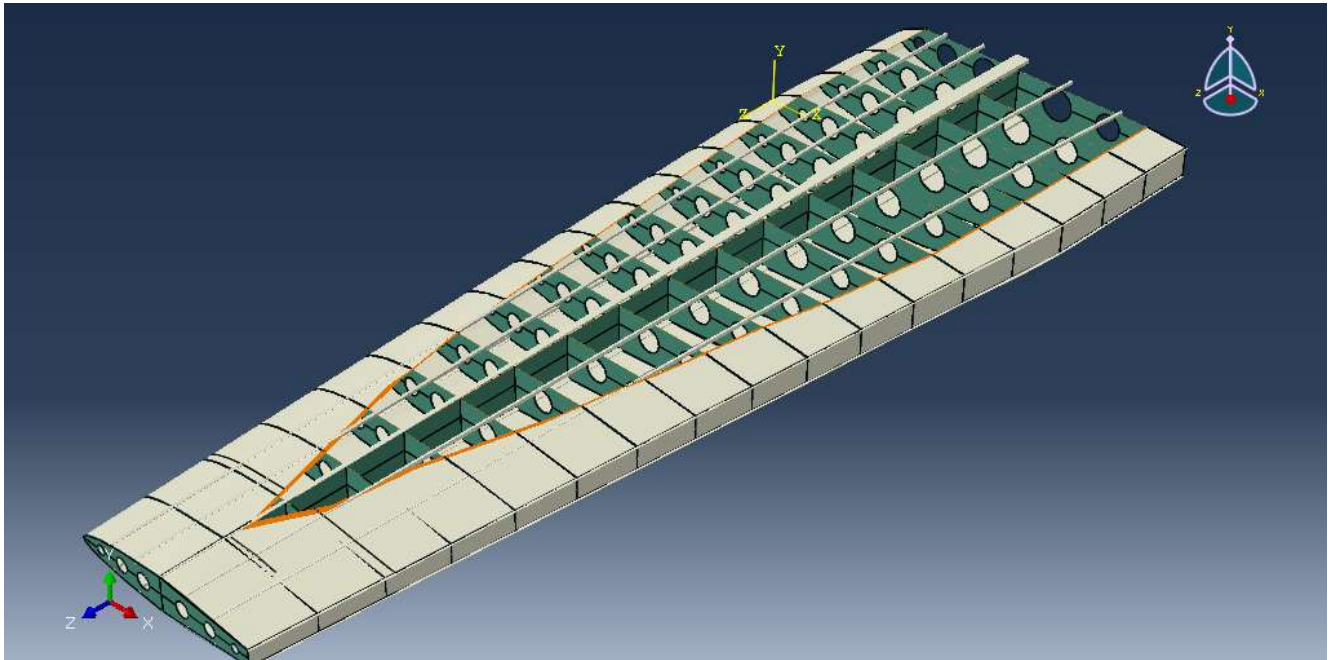


Fig15. Assembly of wing structure

Sixthly, in **Step** module, create the static analysis step.

Seventhly, in **Interaction** module, create the tie restraints using surface-to-surface restraint for the rib and skin, stringer and skin.

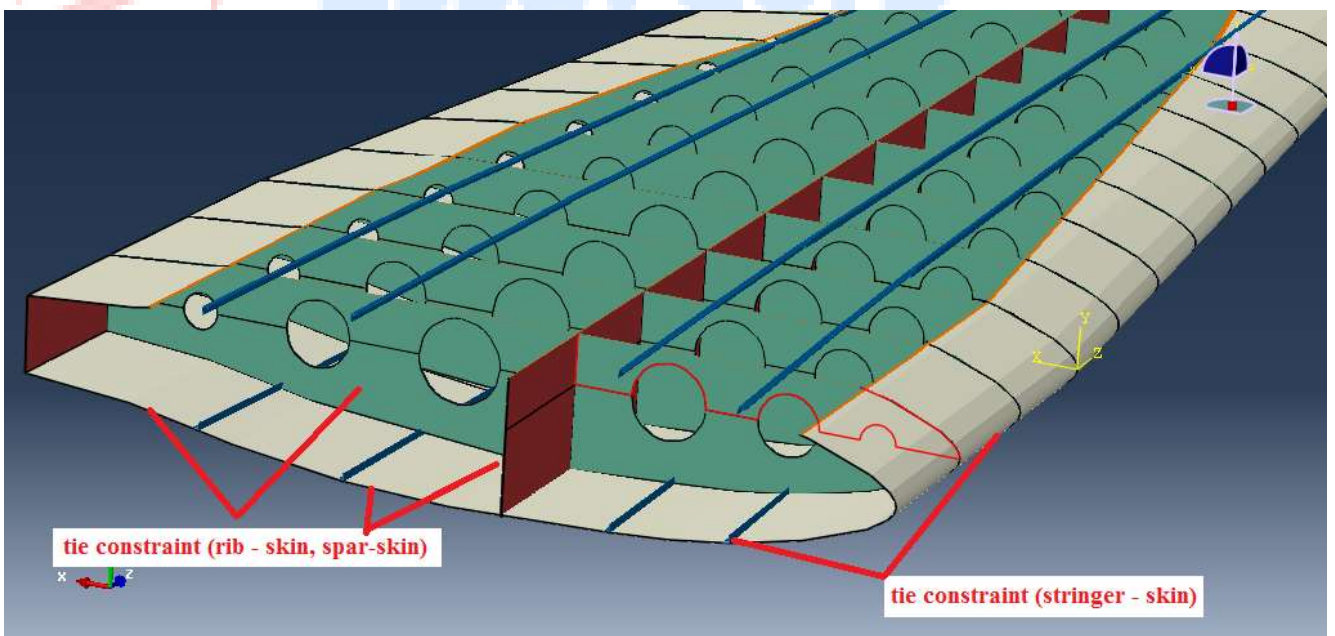


Fig16. Tie restraints between the wing components

Eighthly, in **Mesh** module, create the FE mesh for whole structure. Total element counter is about 100000 with S4R (linear quadrilateral, reduced integral, shell element), S3 (linear triangular shell element), B31 (linear beam element).

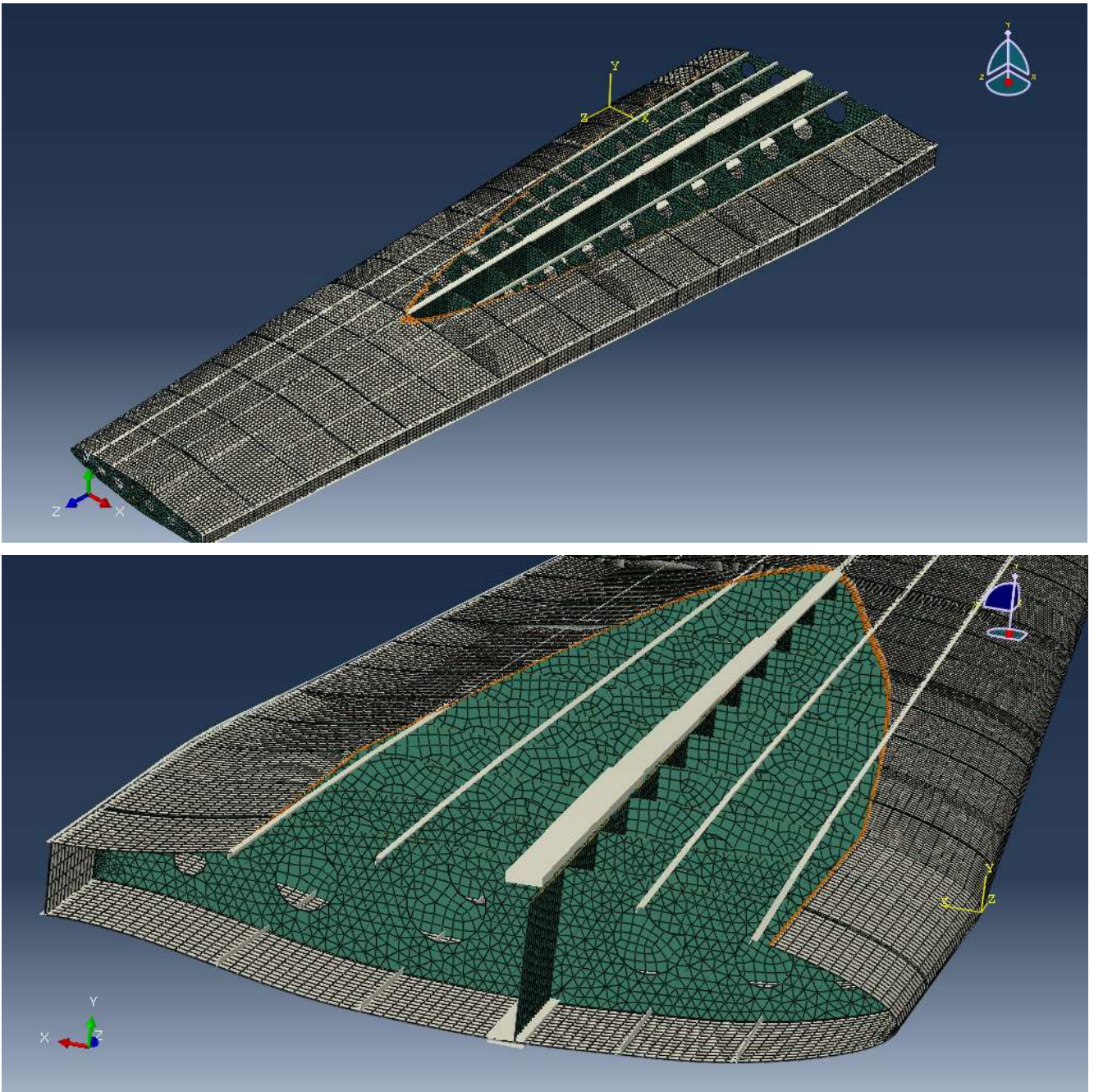


Fig17. FE meshing

Ninthly, in **Load** module, apply the boundary condition and displacement loading following to the experimental conditions (Figure 18). The all dofs of the nodes on the end rib surface and skin surface from the end rib to second are constrained.

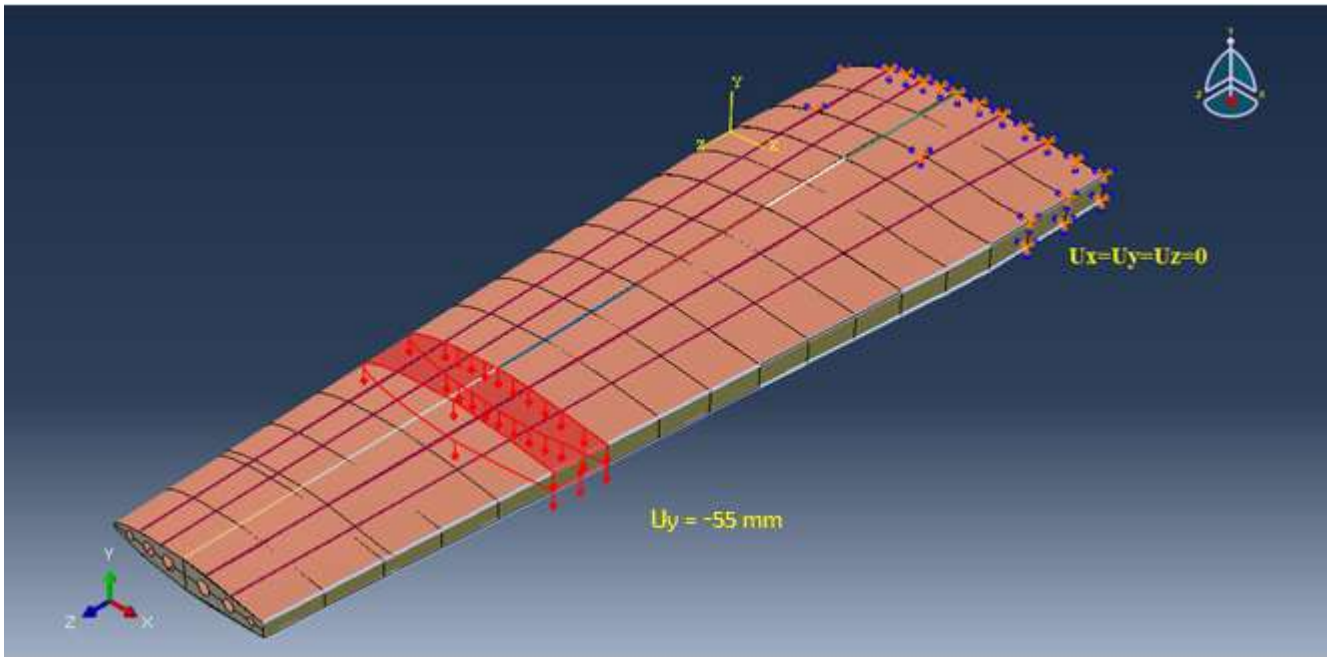


Fig18. Boundary condition

3. Discussion

The global static stress analysis of PC-9 wing structure under the displacement load was performed based on the three-dimensional finite element analysis model as discussed above. The wing root part was fixed and the displacement force of 55 mm was applied at the position of 2/3 of whole wing.

Figure 19 shows the global result of static stress analysis of PC-9 wing structure under the displacement load. And Figure 20 shows the distribution of Von-Mises stress at the interior parts of wing structure including rib, stringer, front and rear spar.

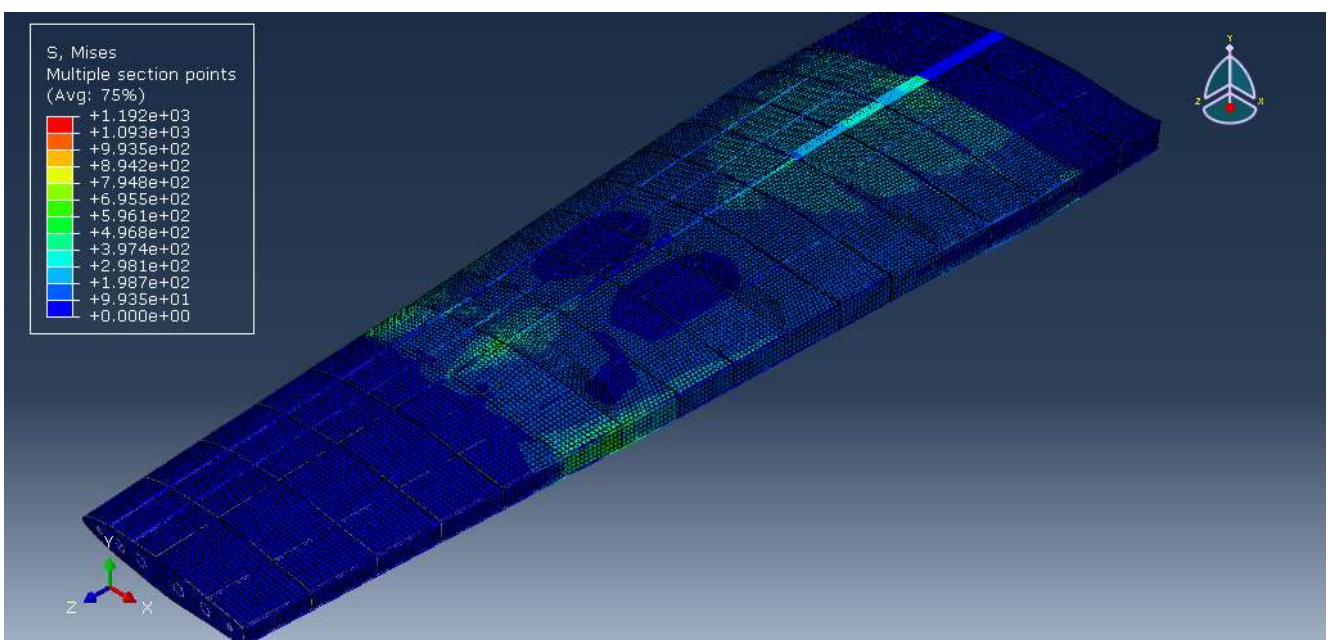


Fig19. FE analysis results

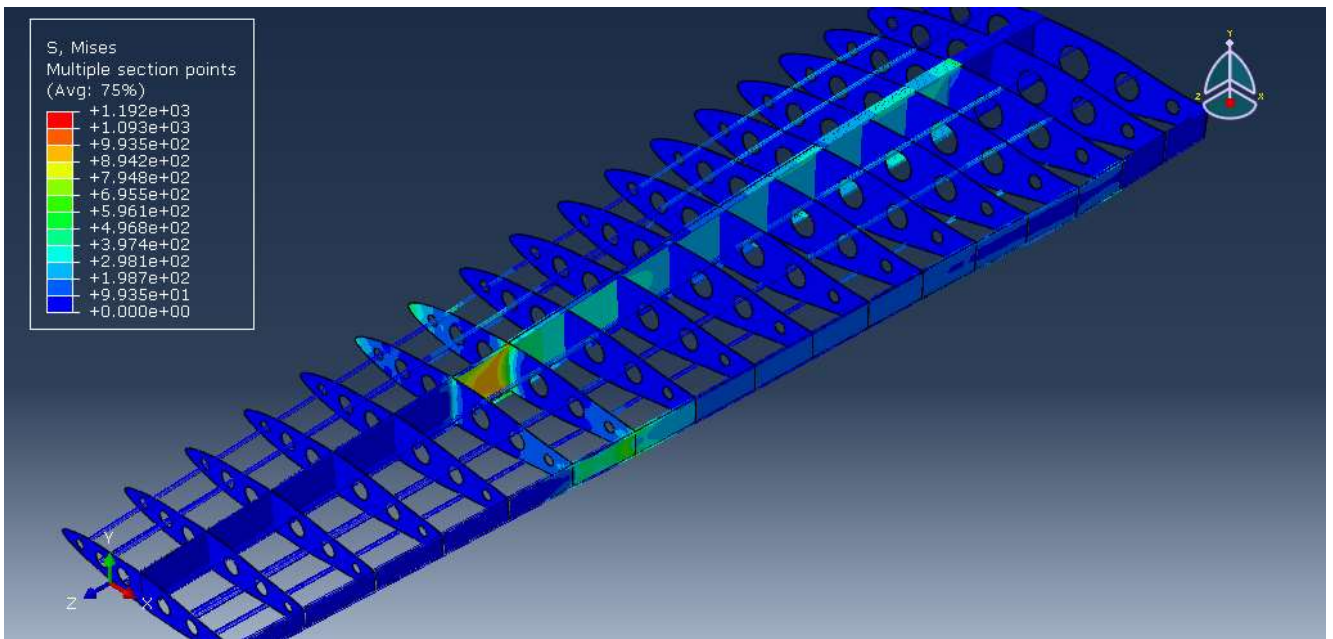


Fig20. Stress field at inner components of wing

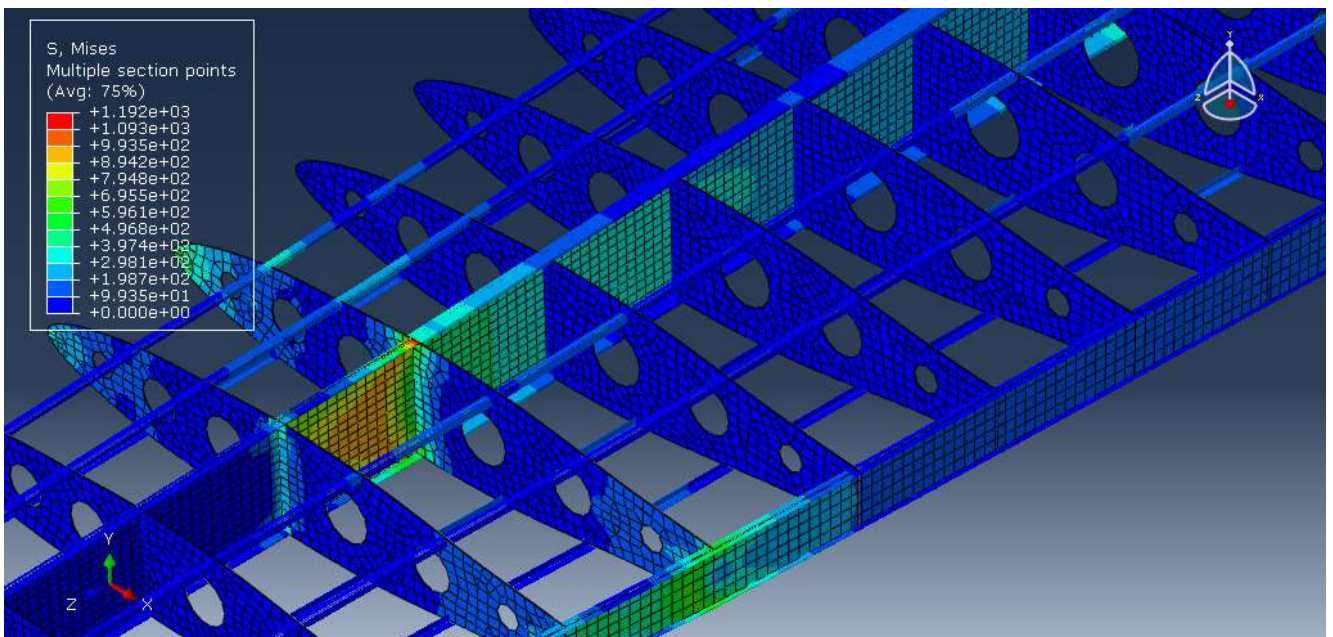


Fig21. Von-Mises stress plot at multiple sections

Consideration of results at individual components:

- Rib

Figures 22, 23 and 24 shows deflection, von-Mises stress and principle strain at wing ribs, respectively.

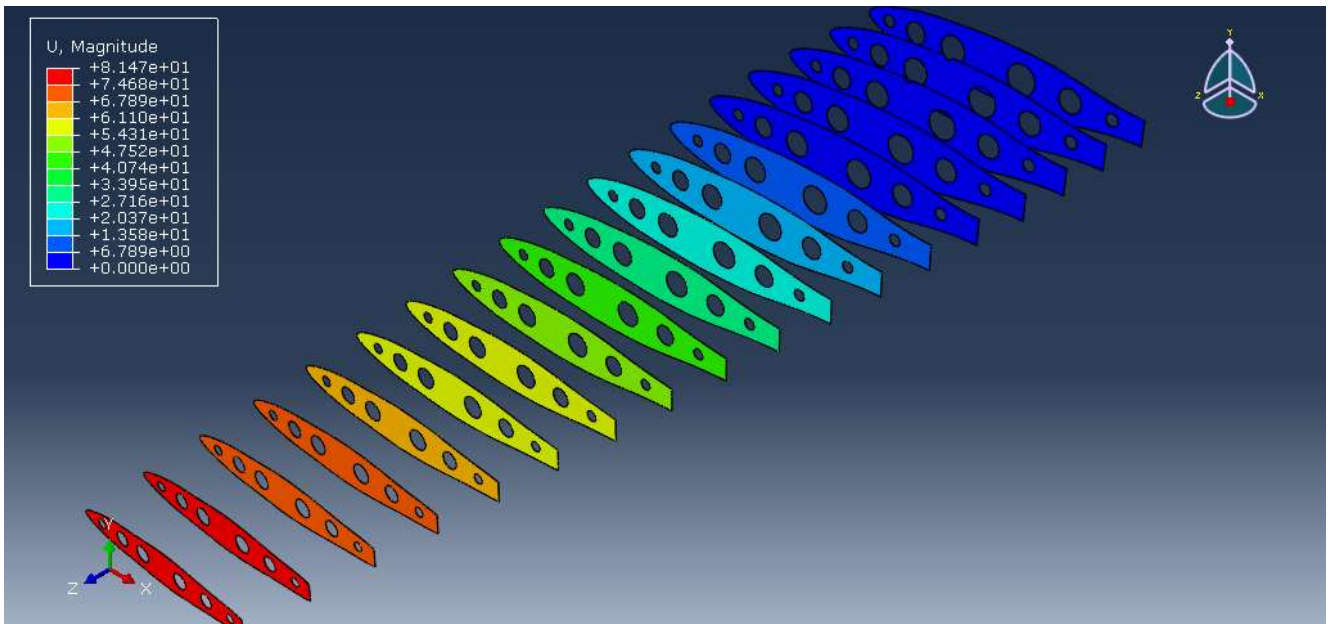


Fig22. Deflection at wing ribs

From the above figure, it is observed that the deflection becomes to be larger from one end of wing to wing tip. Also, the ribs around the loading point are carried out more load as seen from Figure 23.

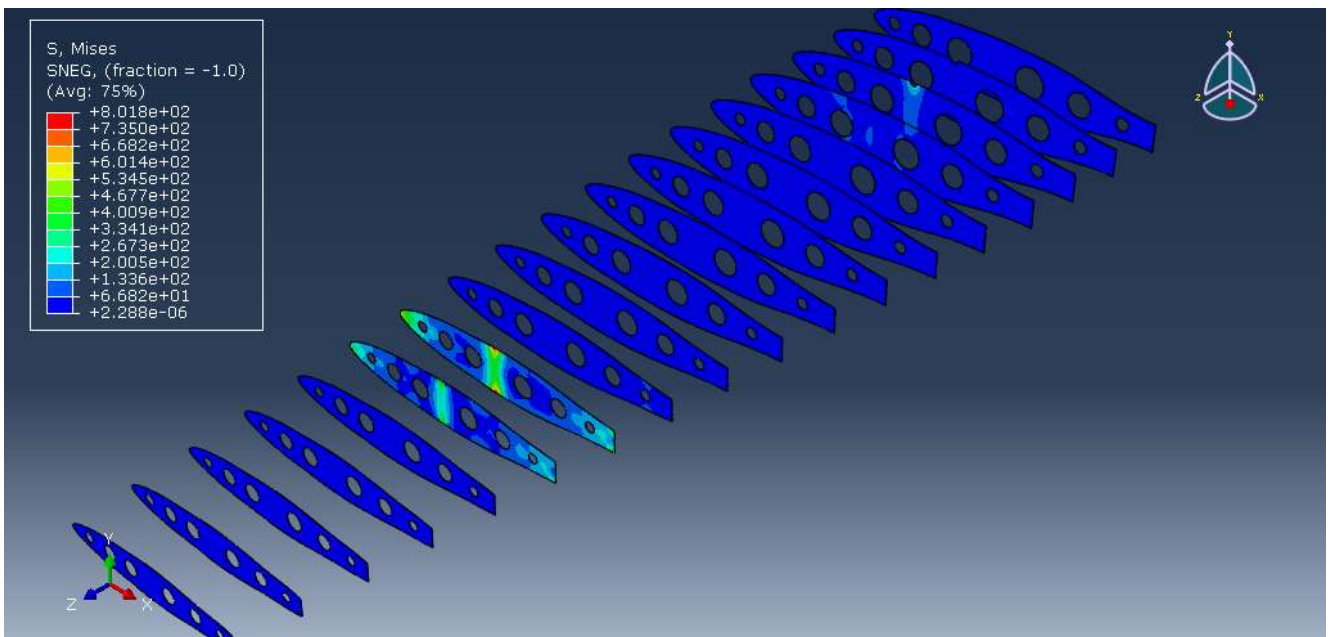


Fig23. Von-mises stress at wing ribs

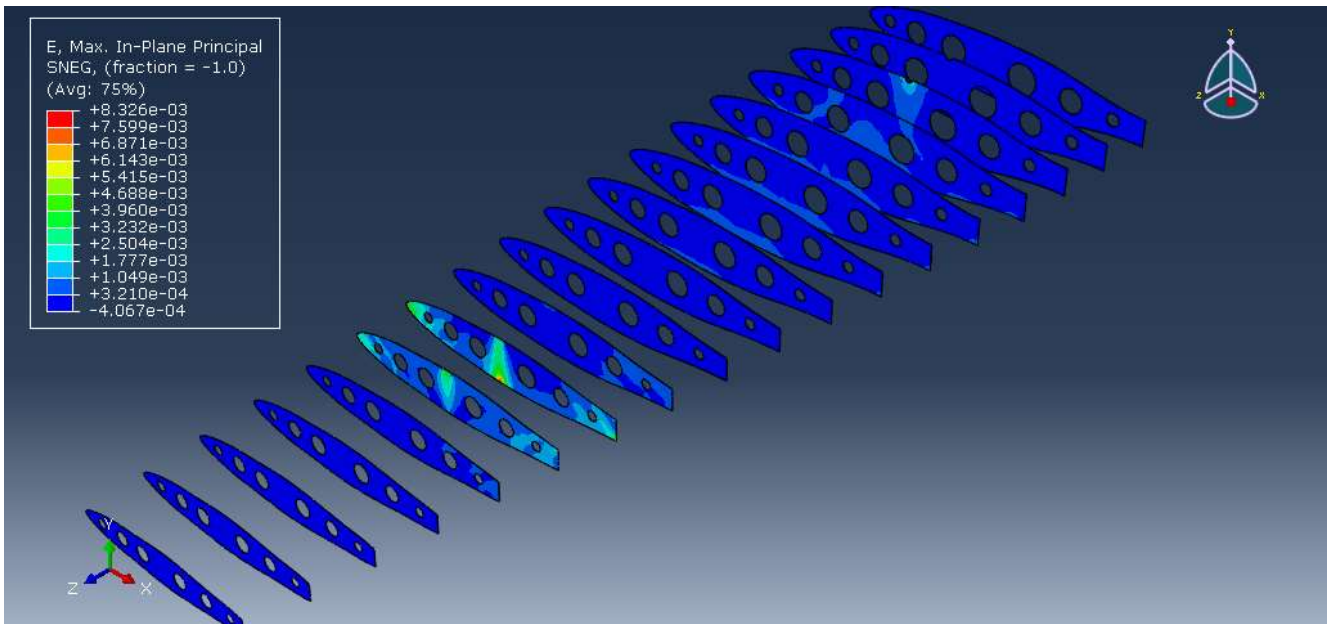


Fig24. Principle strain at wing ribs

- Front spar

Figures 25 and 26 shows von-Mises stress and deflection at front spar, respectively. Front spar at wing is a main load carrying out member. As can be seen from Figure 25, the stress at front spar is higher compared with other members relatively. It shows that front spar is a main load carrying out member at wing. Specially, the stresses at the area of loading point and the fixed area of wing are highest.

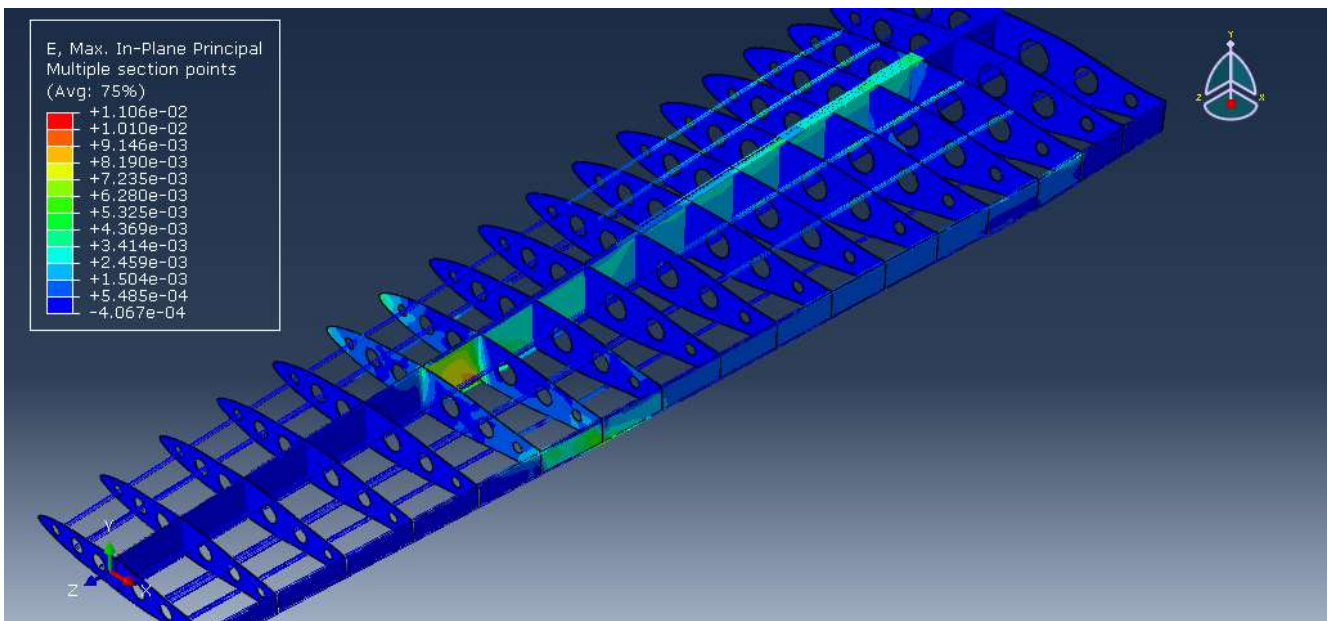


Fig25. Von-Mises stress at front and rear spar

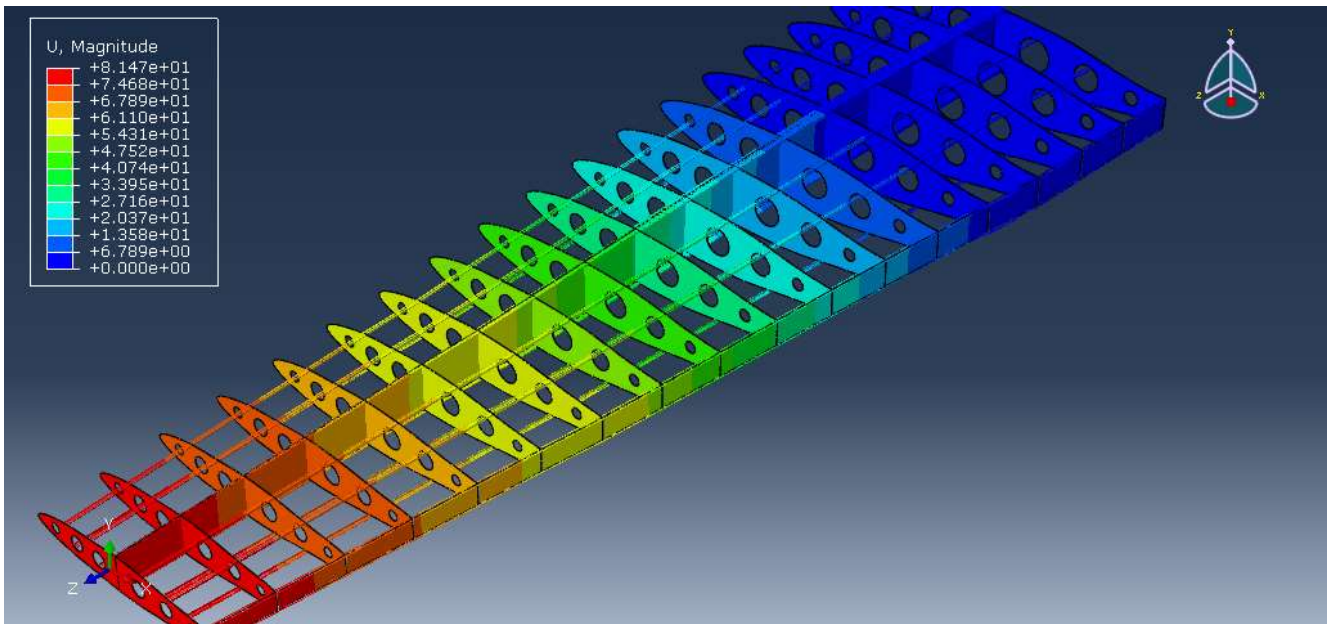


Fig26. Deflection at front and rear spar

- Wing stringer

Figures 27 and 28 shows deflection and von-Mises stress at wing stringer, respectively. It is obtained the results similar to at ribs i.e. the deflection becomes to be larger from one end of wing to wing tip. Also, the stress around the loading point is larger than other areas of wing stringer as seen from Figure 28.

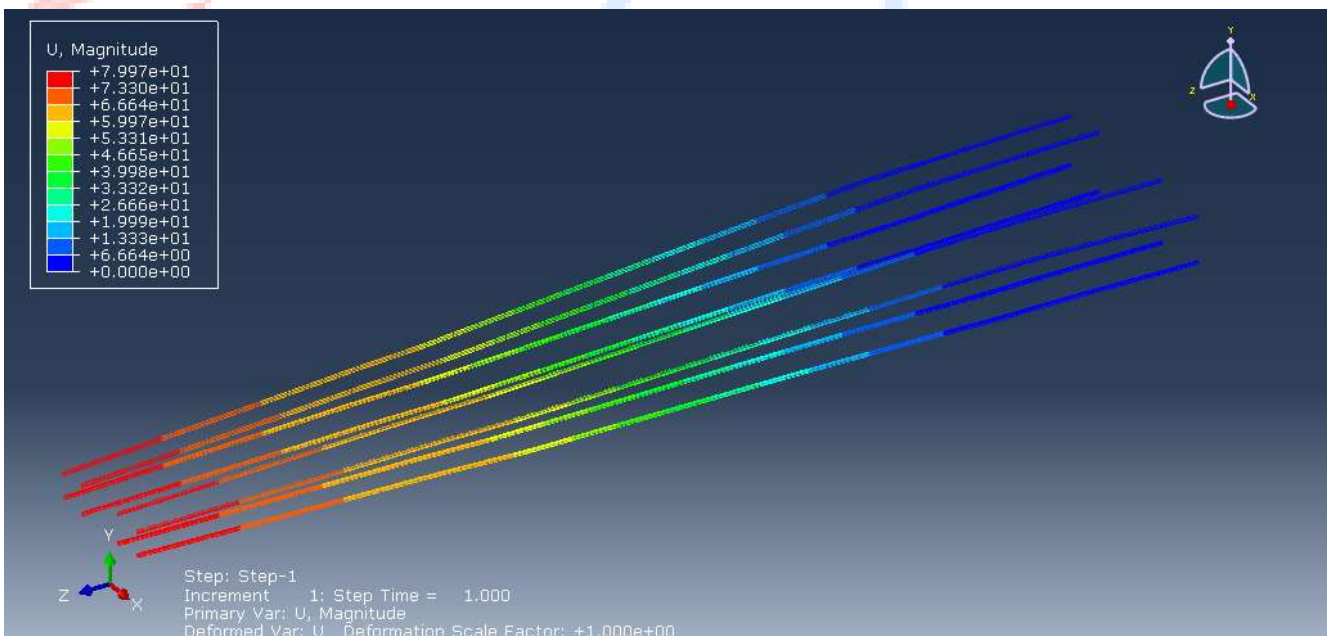


Fig27. Deflection at stringers

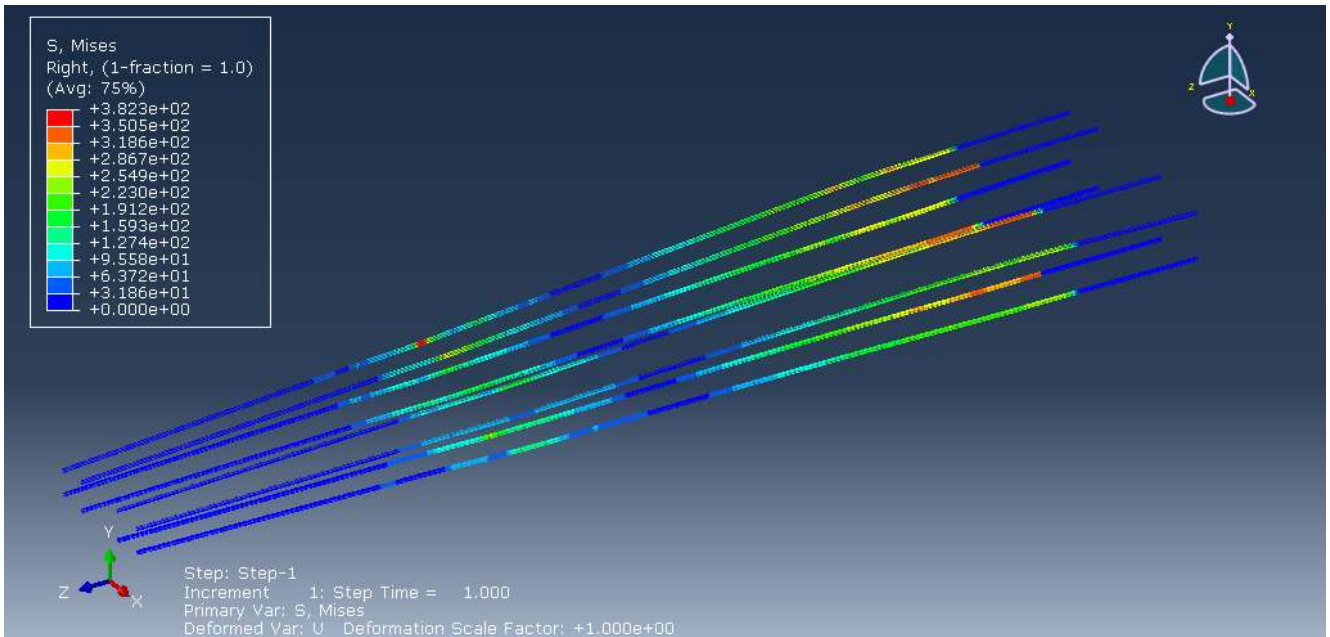


Fig28. Von-Mises stress at stringers

-Wing skin

Figures 29 and 30 shows von-Mises stress and deflection at wing skin, respectively. As mentioned before, the skin makes the appearance of the wing and is connected to stringer. It only plays to transfer aerodynamic distributed load to stringers.

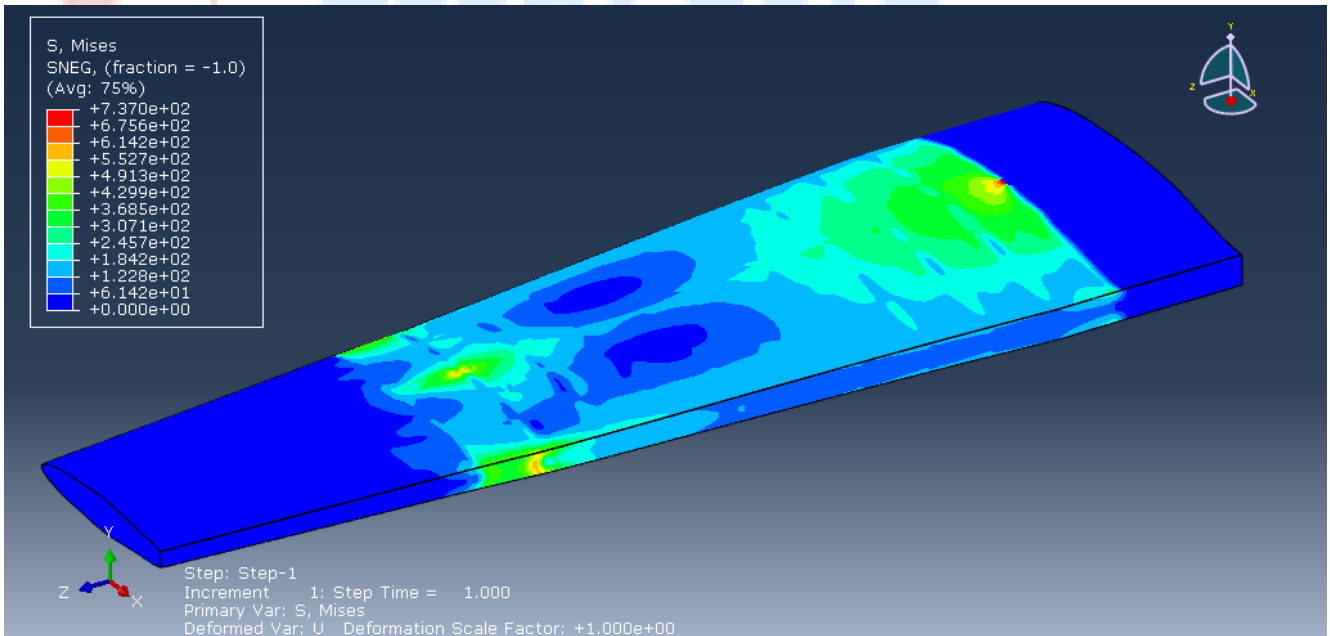


Fig29. Von-Mises stress at wing skin

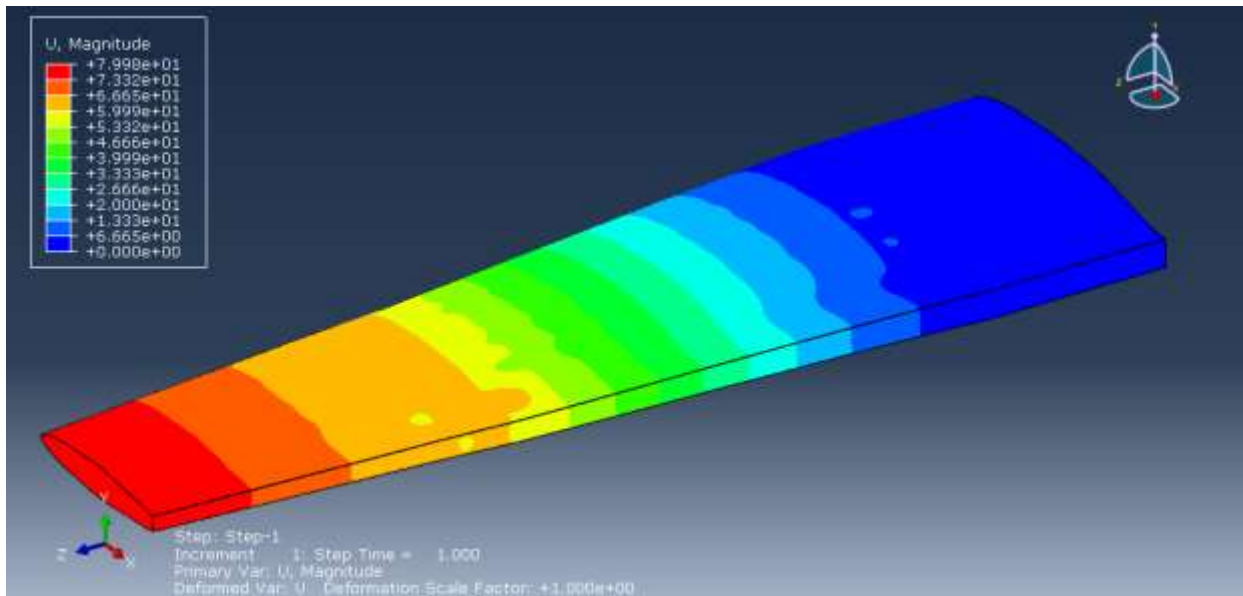


Fig30. Deflection at wing skin

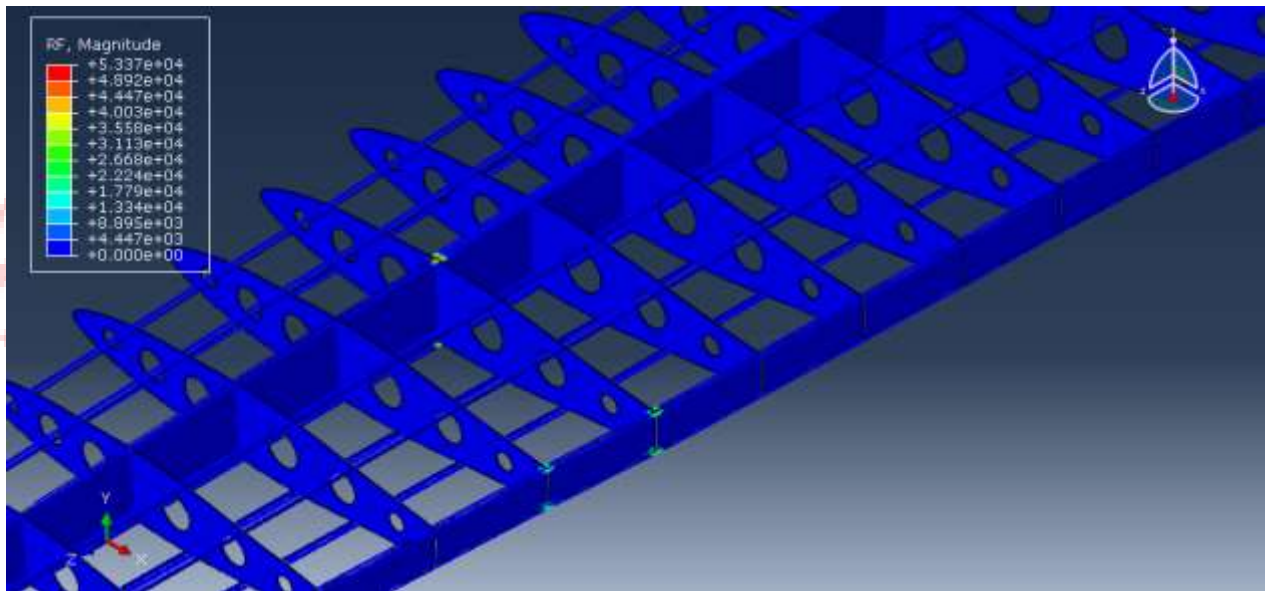


Fig31. Maximum force carrying positions

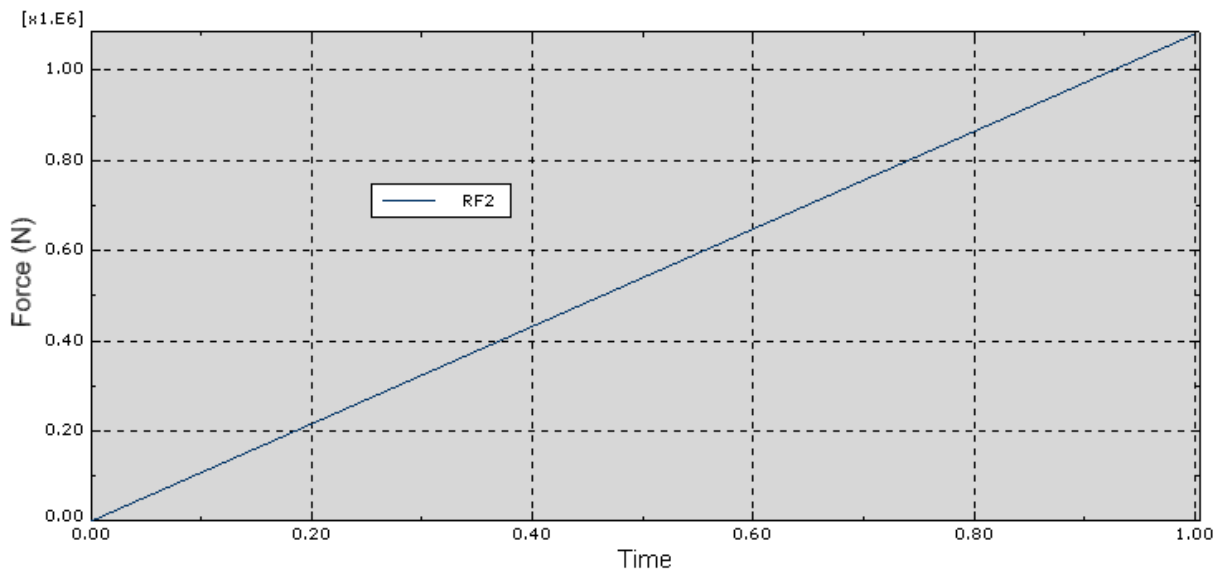


Fig32. Maximum force carrying positions

Figure 33 and 34 shows the final deflection of wing end and the deflection curve, respectively.

Table 1 lists the comparison of deflection of wing end predicted by the finite element analysis with experimental data.

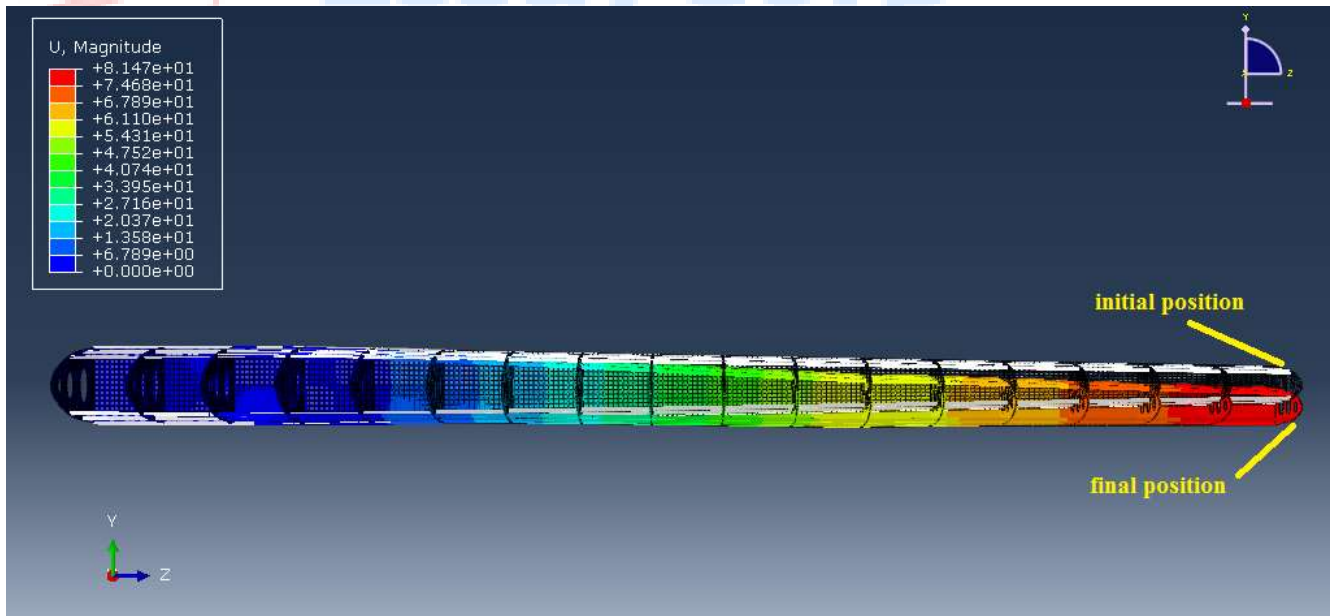


Fig33. Final deflection state

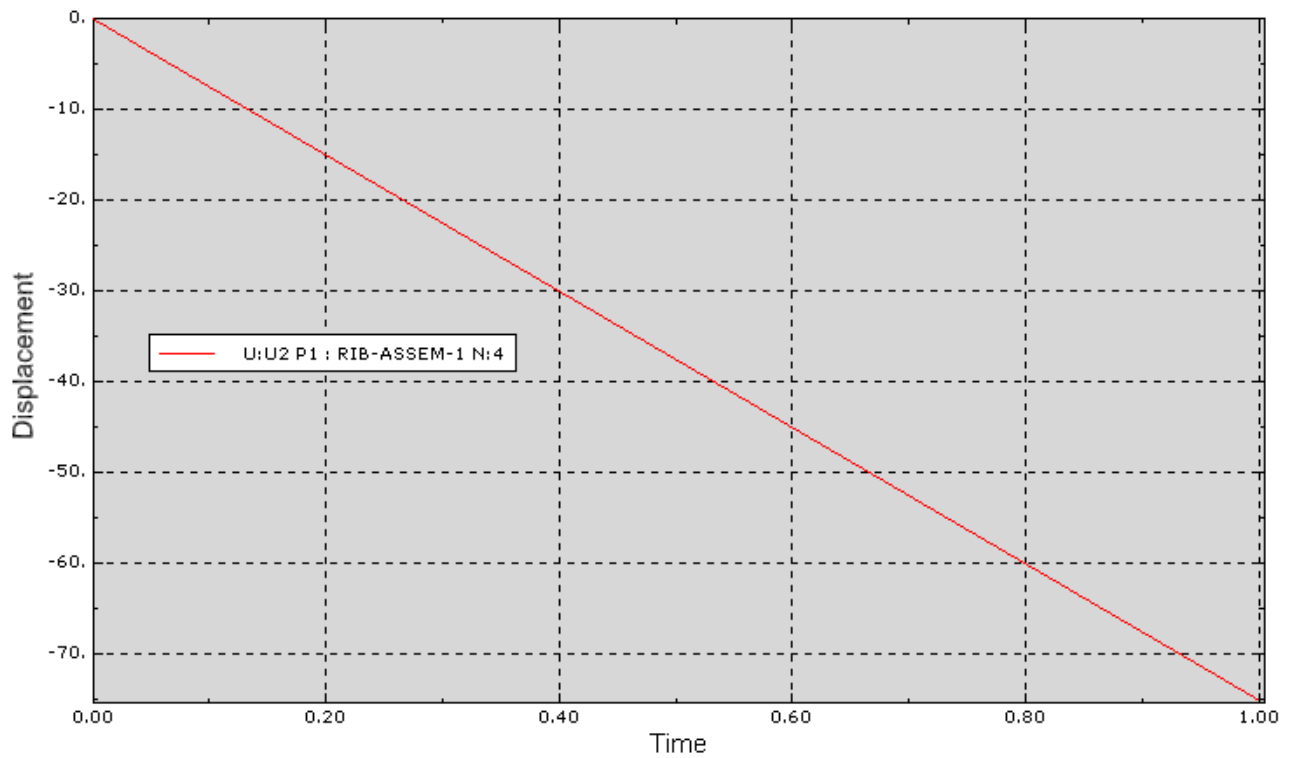


Fig34. Deflection curve at wing tip



EssayCorp 5 years ★★★★★

Table 1. Results compare between experiment and FE simulation

Displacement Loading (mm)	Force at leading edge (KN)	Applied (Reaction) Load (KN)	Displacement at wing tip (mm)	
	experiment	FEM	experiment	FEM
20	2.53	4E3	39	29
40	4.10	8E3	67	55
55	5.97	1.08E3	96	75.2

From table 1, one can know that the deflection and stress of wing end predicted by the finite element analysis have some differences with the experimental data.

Main factors that influences on the numerical error can be reviewed as follows.

First, the geometry used for the finite element analysis has some differences with actual structure of wing due to the complexity of whole wing structure. In the ABAQUS geometry, size and position of wing ribs and internal holes were determined by the linear interpolation. In general, wing stringers only play a role for protecting the outer skin of wing and do not have effects on the force carrying capacity of wing structure.

Second, constitutive relation of material is one of main factors characterizing the global deflection of wing structures. The spar of wing structure is the main part of force carrying capacity and is originally different with outer skin or rib. But the finite element analysis assumes that material of all parts follows the linear elasticity due to the lack of detailed material information. Meanwhile, actual material may exhibit the elastic-plastic hardening under the given loading

Third, the boundary conditions are also one of main factors that influence on the numerical error. The current finite element model used the approximate position of fixed displacement and loading.

Conclusions

This thesis describes determination of the deflections and stresses in a loaded Pilatus PC/9 wing using finite element computational modeling. The procedures of finite element modeling process of the Pilatus PC/9 wing using commercial finite element analysis software ABAQUS and some important topics are discussed. The results of finite element analysis agree with experiment results well.

Works in the future

There is an encountered problem that FE analysis in this work requires a important great time and workforce for creation and improvement of the finite element numerical model. In addition, it is one of the major difficulties in practical implement of the FE approach. Therefore, it is needed the other methods to achieve high-quality and automated FE modeling. One most effective method is the method of finite element parametric modeling. The layout of wing structure, geometric dimension, and FE model including FE meshing and material properties are established parametrically and automatically updated here. Also, the generation processes of FE model of wing structures including geometric and meshing model are advanced based on parametric computer aided designs. The method defines a series of problems of geometric model description, parameter association, and automatic update of the model in the FE numerical modeling process which establishes a key technical basis for

parametric FE simulation and optimization.

Referencing

1. Guan ZQ, Gu YX. A parameterized method for 3D FE modeling based on CAD/CAE integration. *Computer Integr Manu Syst* 2003;12(9):1112–9 Chinese.
2. van Tooren NM. Automated FE analysis in a knowledge based engineering environment. 2006. Report No.: AIAA-2006-947.
3. Xi P, Zhang BY, Ning T. Intelligent product design based on open knowledge representation. *Acta Aeronautica et Astronautica Sinica* 2012;33(9):1746–54 Chinese.
4. Sensmeier M, Samareh J. Automatic aircraft structural topology generation for multidisciplinary optimization and weight estimation. 2005. Report No.: AIAA-2005-1893.
5. Anemaat WA, Schueler KL. Airplane layout design using objectoriented methods. 1997. Report No.: AIAA-1997-5510.
6. Feng HC, Luo MQ, Liu H, Wu Z. A knowledge-based and extensible aircraft conceptual design environment. *Chin J Aeronaut* 2011;24(6):709–19.
7. La Rocca G, van Tooren MJL. Knowledge-based engineering method to support aircraft multidisciplinary design and optimization. *J Aircraft* 2009;46(6):1875–85.
8. Luo MQ, Feng HC, Liu H, Wu Z. Rapid wing structure design and automated scheme control for civil aircraft. *J Beijing Univ Aeronaut Astronaut* 2009;35(4):468–71 Chinese.
9. Luo MQ, Feng HC, Liu H, Wu Z. Rapid wing structural FE modeling and automated control. *J Beijing Univ Aeronaut Astronaut* 2011;37(6):680–4 Chinese.
10. Sun XS, Chen WP, Chen HX. Design oriented FE modeling to aeronautical structures. *Acta Aeronautica et Astronautica Sinica* 1998;19(4):509–12 Chinese.
11. George PL, Seveno E. The advancing-front mesh generation method revisited. *Int J Numer Meth Eng* 1994;37(21): 3605–19.
12. La Rocca G, Michel JL. A knowledge based engineering method to support automatic generation of FE models in aircraft design. In: 45th AIAA aerospace sciences meeting and exhibit; 2007.
13. Perez RE, Chung J, Behdinan K. Aircraft conceptual design using genetic algorithms. 2000.

Report No.: AIAA-2000-4938.

14. Yu YY, Chen M. New method for ship FE method pre-processing based on 3D parametric technique. J Mar Sci Technol 2009;14(3):398–407 Chinese.
15. Lee KY, Kim LL, Kim TW. An algorithm of automatic 2D quadrilateral mesh generation with line restraints. Comput Aided Des 2003;35:1055–68.
16. Liu H, Tian YL, Zhang CY, Yin J, Sun YJ. Evaluation model of design for operation and architecture of hierarchical virtual simulation for flight vehicle design. Chin J Aeronaut 2012;25(2):216–26.
17. Li H, Li XN, Chen GD. A method for mesh generation of all quadrilateral FEs-improved pattern module method. Chin J Comput Mech 2002;19(1):16–9 Chinese.
18. Peng RY, Wang HP, Wang ZP, Lin Y. Decision-making of aircraft optimum configuration utilizing multi-dimensional game theory. Chin J Aeronaut 2010;23(2):194–7.
19. ABAQUS/CAE v6.14 User Manual
20. SolidWorks v2010 User Manual

Related Topics :

[Aerospace Engineering Assignment Help](#)

[Engineering Assignment Help](#)